RSC Advances

PAPER

View Article Online
View Journal | View Issue

Open Access Article. Published on 18 September 2018. Downloaded on 11/8/2025 3:33:28 AM.
This article is licensed under a Creative Commons Attribution-NonCommercial 3.0 Unported Licence.

Check for updates

Cite this: *RSC Adv.*, 2018, **8**, 32269

Role of C, S, Se and P donor ligands in copper(I) mediated C–N and C–Si bond formation reactions†

Katam Srinivas and Ganesan Prabusankar *

The first comparative study of C, S, Se and P donor ligands-supported copper(I) complexes for C–N and C–Si bond formation reactions are described. The syntheses and characterization of eight mononuclear copper(I) chalcogenone complexes, two polynuclear copper(I) chalcogenone complexes and one tetranuclear copper(I) phosphine complex are reported. All these new complexes were characterized by CHN analysis, FT-IR, UV-vis, multinuclear NMR and single crystal X-ray diffraction techniques. The single crystal X-ray structures of these complexes depict the existence of a wide range of coordination environments for the copper(I) center. This is the first comparative study of metal–phosphine, metal–NHC and metal–imidazolin-2-chalcogenones in C–N and C–Si bond formation reactions. Among all the catalysts, mononuclear copper(I) thione, mononuclear copper(I) N-heterocyclic carbene and tetranuclear copper(I) phosphine are exceedingly active towards the synthesis of 1,2,3-triazoles as well as for the cross-dehydrogenative coupling of alkynes with silanes. The cross-dehydrogenative coupling of terminal alkynes with silanes represents the first report of a catalytic process mediated by metal–imidazolin-2-chalcogenones.

Received 16th July 2018
Accepted 31st August 2018

DOI: 10.1039/c8ra06057f

rsc.li/rsc-advances

Introduction

The chemistry of "soft" Lewis donors such as imidazolin-2-chalcogenones (NHC=E, E = S and Se)-supported metal complexes have received much attention in catalysis during the past two decades due to their tuneable σ-donor and π-accepting properties.[1–3] In fact, the electron cloud at the metal centre is responsible for the activities associated with the metal complexes. Thus, the metal will be more electrophilic when attached to more π-acceptor ligands (PPh_3), while, it becomes relatively less electrophilic when attached to weak π-acceptors such as NHC and NHC=E (Chart 1).[4] Notably, the stronger σ-donor abilities over the π-accepting nature of NHC=E compared to both phosphine and NHC is due to the existence of a larger contribution (66%) of the zwitterionic form (NHC^{+}–E^{-}).[5]

Although, the coordination chemistry of transition metals with NHC=E is well known,[6] the catalytic applications of these complexes are limited.[7] Notably, the catalytic efficiency of NHC=E metal complexes is significantly remarkable as compared to NHC–metal complexes (Chart 2).[7] For example, in copper chemistry, NHC=E supported copper(I) complexes {[(**IMS**)$_2$CuCl]; **IMS** = 1,3-dimethylimidazoline-2-thione, and [(**IMes=Se**)$_2$Cu][BF_4]; **IMes=Se** = 1,3-bis(2,4,6-trimethylphenyl)imidazolin-2-selone} were found to be more regioselective in the hydroborylation of alkynes over NHC–Cu.[7d,e] Recently, we investigated the efficiency of [(**Bptp**/**Bpsp**)$_{12}$Cu$_8$][PF_6]$_8$ (**Bptp** = 2,6-bis(1-isopropylimidazole-2-thione)pyridine and **Bpsp** = 2,6-bis(1-isopropylimidazole-2-selone)pyridine) in click catalysis as well as in the hydroamination of alkynes, and they were found to be as good as the NHC–Cu catalyst.[8] However, to the best of our knowledge the catalytic comparisons of phosphine–copper, NHC–copper and NHC=E–copper have never been investigated.

Herein, we present the first comparative study of phosphine–copper, NHC–copper and NHC=E–copper. The coordination properties of ligands, structural features of copper(I) complexes and catalytic efficiency of new copper(I) complexes are reported in detail. The mononuclear copper(I) complexes (IMes=E)CuX [E = S, Se, IMes=E 1,3-bis(2,4,6-trimethylphenyl)imidazol-2-thone (**1–3**) and 1,3-bis(2,4,6-trimethylphenyl)imidazol-2-selone (**4–5**)], (NHC=E)$_2$CuX, NHC=E; **IMes=Se**, X = $CuCl_2$ (**7**), NHC=E; **IMes=Se**, X = PF_6 (**9**) and NHC=E = **IPr=Se**, X = PF_6 (**11**) [**IPr=**

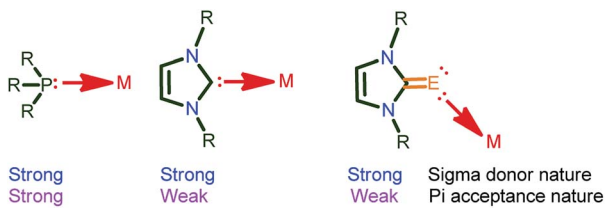

Chart 1 σ-donor and π-accepting nature of PPh_3, NHC and NHC=E ligands.[2]

Department of Chemistry, Indian Institute of Technology Hyderabad, Kandi, Sangareddy, Telangana, India-502 285. E-mail: prabu@iith.ac.in; Fax: +91 40 2301 6032; Tel: +91 40 2301 6089

† Electronic supplementary information (ESI) available: FT-IR, NMR, X-ray data, figures and GC data. ^{1}H and ^{13}C NMR spectra of the synthesized complex. Catalysis protocols and characterization data of catalytic products. CCDC 1855114–1855124. For ESI and crystallographic data in CIF or other electronic format see DOI: 10.1039/c8ra06057f

Open Access Article. Published on 18 September 2018. Downloaded on 11/8/2025 3:33:28 AM.
This article is licensed under a Creative Commons Attribution-NonCommercial 3.0 Unported Licence.

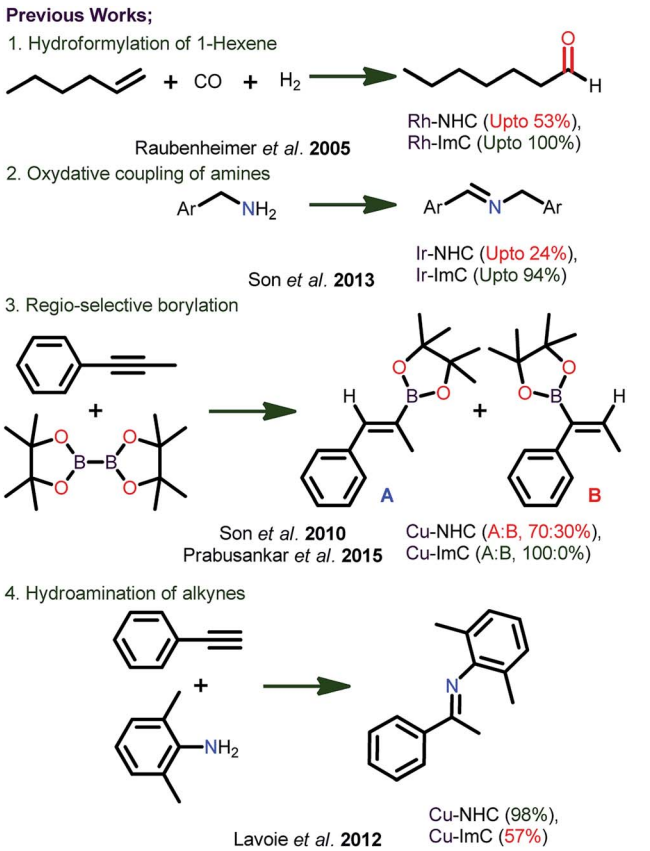

Chart 2 Known catalytic comparisons between NHC=E–metal and NHC–metal-supported Cu(I) complexes.

Se, 1,3-bis(2,6-diisopropylphenyl)imidazoline-2-selone], and polynuclear copper(I) complexes $[(\mathbf{Ebis})CuI]_n$ (**13**) [where **Ebis** = 1,2-bis(3-methyl-4-imidazolin-2-selone)ethane], $[(\mathbf{Ebpis})_{1.5}\text{-}CuBF_4]_n$ (**14**) [**Ebpis** = 1,2-bis(3-isopropyl-4-imidazolin-2-selone) ethane] were isolated. Interestingly, **7**, **9** and **11** can also be isolated from [(IMes)CuCl] (**6**) by the ligand transfer method. Besides, the complexes **13** and **14** were synthesized from the tetranuclear copper(I) complex, $[(PPh_3)_4Cu_4I_4]$ (**12**). Complexes **1–14** were characterized by CHN analysis, FT-IR, multinuclear NMR and single crystal X-ray diffraction techniques.

Experimental

Materials and methods

The necessary manipulations were carried out under an argon atmosphere in a glove box or using standard Schlenk techniques. The solvents were purchased from commercial sources and purified according to standard procedures and freshly distilled under argon atmosphere prior to use.[9] **IMes·HCl** (1,3-dimesityl-1*H*-imidazol-3-ium chloride), **IMes=S** (1,3-dimesityl-1*H*-imidazole-2(3*H*)-thione), **IMes=Se** (1,3-dimesityl-1*H*-imidazole-2(3*H*)-selenone), **IPr=Se** (1,3-bis(2,6-diisopropylphenyl)-1*H*-imidazole-2(3*H*)-selenone), **Ebis** (3,3′-(ethane-1,2-diyl)bis(1-methyl-1*H*-imidazole-2(3*H*)-selenone)) and **Ebpis** (3,3′-(ethane-1,2-diyl)bis(1-isopropyl-1*H*-imidazole-2(3*H*)-selenone)) were prepared as previously reported (Chart 3).[7k,l] Unless otherwise stated, the chemicals were purchased from commercial sources. CuCl, CuBr, CuI, $[Cu(CH_3CN)_4]PF_6$, KPF_6 and NH_4BF_4 were purchased from Sigma Aldrich and used as received.

FT-IR measurement (neat) was carried out on a Bruker Alpha-P Fourier transform spectrometer. The UV-vis spectra were obtained on a T90+ UV-visible spectrophotometer. NMR spectra were recorded on a Bruker Ultrashield-400 spectrometer at 25 °C unless otherwise stated. Chemical shifts are given relative to TMS and were referenced to the solvent resonances as internal standards. Elemental analyses were performed by the Euro EA-300 elemental analyzer. The crystal structures of **1–5**, **7**, **9**, **11**, **13** and **14** were obtained on an Oxford Supernova diffractometer. Single crystals of complexes suitable for the single crystal X-ray analysis were mounted on a Goniometer KM4/Xcalibur equipped with a Sapphire 2 (large Be window) detector (CuKα radiation source, $\lambda = 1.5418$ Å) at ambient temperature (298 K) in inert oil. Using Olex2,[10] the structure was solved with the ShelXS[11] structure solution program using Direct Methods and refined with the Olex2 refine refinement package using Gauss–Newton minimization. Absorption corrections were performed on the basis of multi-scans. Non-hydrogen atoms were anisotropically refined. H atoms were included in the refinement in calculated positions riding on their carrier atoms. No restraint was made for any of the compounds. Due to the severely disordered (positional disorder) imidazole ring with $U_{eq} > 0.2$, molecule **14** gave "B" level alerts and atoms are not shown in the ellipsoid view for clarity.

Synthesis of 1

A mixture of **IMes=S** (0.100 g, 0.297 mmol) and CuCl (0.035 g, 0.356 mmol) in methanol (5 mL) was refluxed at 80 °C for 12 h. The clear solution was then brought to ambient temperature to form colorless crystals of **1**. Yield: 78% (based on CuCl). Mp: 207–209 °C (decomposed). Elemental analysis calcd (%) for $C_{21}H_{24}ClCuN_2S$ (435.50): C, 57.92; H, 5.55; N, 6.43; found: C, 57.84; H, 5.57; N, 6.39. ^{1}H NMR (400 MHz, DMSO-d_6): $\delta = 7.66$ (s, 2H, Im*H*), 7.07 (s, 4H, CH_{meta}), 2.26 (s, 6H, CH_{3para}), 1.95 (s, 12H, CH_{3ortho}). ^{13}C NMR (100 MHz, DMSO-d_6): $\delta = 155.66$ (*C*=S), 140.04, 134.65, 131.85, 129.61, 121.67 (Ar*C*), 20.69 (*p*-CH_3), 17.11 (*o*-CH_3). FT-IR (neat): $\bar{\nu}$ = 3148(w), 3112(w), 3082(w), 2917(m), 1605(m), 1558(w), 1482(s), 1449(m), 1382(s), 1290(m), 1235(s), 1167(w) (C=S), 1140(w), 1034(m), 925(w), 853(s), 750(s), 693(s), 666(w), 606(m), 572(m), 520(m) cm^{-1}.

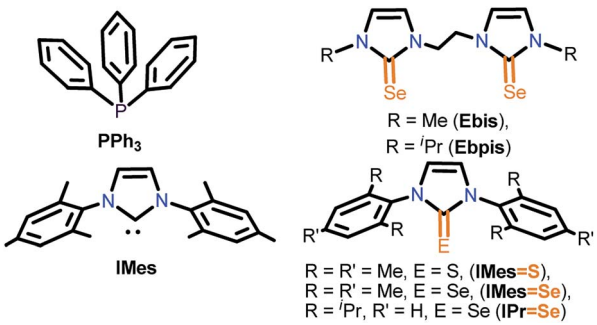

Chart 3 Types of ligands studied for copper(I)-mediated 1,3-dipolar cycloaddition of alkynes with azides.

Open Access Article. Published on 18 September 2018. Downloaded on 11/8/2025 3:33:28 AM.
This article is licensed under a Creative Commons Attribution-NonCommercial 3.0 Unported Licence.

Synthesis of 2

Complex **2** was prepared in the same manner as described for **1** using IMes=S (0.100 g, 0.297 mmol) and CuBr (0.051 g, 0.356 mmol) in methanol (5 mL). Yield: 84% (based on CuBr). Mp: 220–222 °C (decomposed). Elemental analysis calcd (%) for $C_{21}H_{24}BrCuN_2S$ (479.93): C, 52.55; H, 5.04; N, 5.84; found: C, 52.54; H, 5.07; N, 5.79. ^{1}H NMR (400 MHz, DMSO-d_6): δ = 7.31 (s, 2H, Im*H*), 6.97 (s, 4H, C*H*$_{meta}$), 2.22 (s, 6H, C*H*$_{3para}$), 1.93 (s, 12H, C*H*$_{3ortho}$). ^{13}C NMR (100 MHz, DMSO-d_6): δ = 159.87 (*C*=S), 138.59, 135.02, 133.21, 128.87, 119.70 (Ar*C*), 20.62 (*p*-*C*H$_3$), 17.32 (*o*-*C*H$_3$). FT-IR (neat): $\bar{\nu}$ = 3147(w), 3113(w), 3084(w), 2916(m), 1604(m), 1556(w), 1481(s), 1449(m), 1382(s), 1345(w), 1289(m), 1234(s), 1167(w) (C=S), 1141(w), 1033(m), 924(w), 885(s), 851(m), 748(s), 693(s), 644(w), 605(m), 573(m), 519(m) cm^{-1}.

Synthesis of 3

A mixture of IMes=S (0.100 g, 0.297 mmol) and CuI (0.068 g, 0.356 mmol) in methanol (5 mL) was refluxed at 80 °C for 12 h. The resulting white precipitate was dissolved in hot acetonitrile and allowed to crystallize under ambient conditions over 2 days. Yield: 71% (based on CuI). Mp: 232–234 °C (melting). Elemental analysis calcd (%) for $C_{21}H_{24}CuIN_2S$ (526.95): C, 47.87; H, 4.59; N, 5.32; found: C, 47.84; H, 4.57; N, 5.29. ^{1}H NMR (400 MHz, DMSO-d_6): δ = 7.61 (s, 2H, Im*H*), 7.08 (s, 4H, C*H*$_{meta}$), 2.28 (s, 6H, C*H*$_{3para}$), 1.98 (s, 12H, C*H*$_{3ortho}$). ^{13}C NMR (100 MHz, DMSO-d_6): δ = 156.55 (*C*=S), 139.76, 134.78, 132.17, 129.50, 121.27 (Ar*C*), 20.69 (*p*-*C*H$_3$), 17.23 (*o*-*C*H$_3$). FT-IR (neat): $\bar{\nu}$ = 3145(w), 3111(w), 3084(w), 2913(m), 1597(m), 1556(w), 1478(s), 1445(m), 1380(s), 1286(m), 1230(s), 1165(w) (C=S), 1138(w), 1028(m), 921(w), 848(s), 743(s), 690(s), 604(m), 570(m) cm^{-1}.

Synthesis of 4

Complex **4** was prepared in the same manner as described for **1** using **IMes=Se** (0.100 g, 0.260 mmol) and CuBr (0.048 g, 0.312 mmol) in methanol (5 mL). Yield: 87% (based on CuBr). Mp: 227–229 °C (melting). Elemental analysis calcd (%) for $C_{21}H_{24}BrCuN_2Se$ (526.85): C, 47.88; H, 4.59; N, 5.32; found: C, 47.91; H, 4.57; N, 5.29. ^{1}H NMR (400 MHz, DMSO-d_6): δ = 7.73 (s, 2H, Im*H*), 7.02 (s, 4H, C*H*$_{meta}$), 2.25 (s, 6H, C*H*$_{3para}$), 1.95 (s, 12H, C*H*$_{3ortho}$). ^{13}C NMR (100 MHz, DMSO-d_6): δ = 148.22 (*C*=Se), 139.24, 134.58, 133.32, 129.13, 123.30 (Ar*C*), 20.68 (*p*-*C*H$_3$), 17.57 (*o*-*C*H$_3$). FT-IR (neat): $\bar{\nu}$ = 3145(w), 3108(w), 3078(w), 2916(m), 1605(m), 1553(w), 1480(s), 1447(m), 1371(s), 1337(w), 1291(m), 1232(s), 1166(w) (C=Se), 1125(w), 1032(m), 925(w), 851(s), 752(s), 688(s), 594(w), 568(s), 520(m) cm^{-1}.

Synthesis of 5

Complex **5** was prepared in the same manner as described for **3** using **IMes=Se** (0.100 g, 0.260 mmol) and CuI (0.060 g, 0.312 mmol) in methanol (5 mL). Yield: 77% (based on CuI). Mp: 224–226 °C (melting). Elemental analysis calcd (%) for $C_{21}H_{24}CuIN_2Se$ (573.85): C, 43.95; H, 4.22; N, 4.88; found: C, 43.91; H, 4.17; N, 4.89. ^{1}H NMR (400 MHz, DMSO-d_6): δ = 7.79 (s, 2H, Im*H*), 7.08 (s, 4H, C*H*$_{meta}$), 2.30 (s, 6H, C*H*$_{3para}$), 1.97 (s, 12H, C*H*$_{3ortho}$). ^{13}C NMR (100 MHz, DMSO-d_6): δ = 149.14 (*C*=Se), 139.85, 134.57, 132.94, 129.53, 123.31 (Ar*C*), 20.77 (*p*-*C*H$_3$), 17.38 (*o*-*C*H$_3$). FT-IR (neat): $\bar{\nu}$ = 3143(w), 3107(w), 3079(w), 2913(m), 1599(m), 1551(m), 1477(s), 1443(m), 1369(s), 1334(w), 1289(m), 1228(s), 1163(w) (C=Se), 1123(m), 1026(m), 922(w), 849(s), 746(s), 684(s), 599(w), 566(m) cm^{-1}.

Synthesis of 7

Method 1. Complex **7** can be prepared in the same manner as described for **1** using **IMes=Se** (0.100 g, 0.260 mmol) and CuCl (0.031 g, 0.312 mmol) in methanol (5 mL). Yield: 75% (based on CuCl).

Method 2. IMes=Se (0.100 g, 0.260 mmol) was treated with excess [(IMes)CuCl] (0.16 g, 0.426 mmol) in acetone under refluxing conditions overnight to yield **7**. Yield: 65% (based on IMesCuCl). Mp: 218–220 °C (melting). Elemental analysis calcd (%) for $C_{42}H_{48}Cl_2Cu_2N_4Se_2$ (964.79): C, 52.29; H, 5.01; N, 5.81; found: C, 52.30; H, 5.07; N, 5.84. ^{1}H NMR (400 MHz, DMSO-d_6): δ = 7.81 (s, 2H, Im*H*), 7.07 (s, 4H, C*H*$_{meta}$), 2.28 (s, 6H, C*H*$_{3para}$), 1.94 (s, 12H, C*H*$_{3ortho}$). ^{13}C NMR (100 MHz, DMSO-d_6): δ = 148.59 (*C*=Se), 140.00, 134.46, 132.76, 129.58, 123.45 (Ar*C*), 20.74 (*p*-*C*H$_3$), 17.21 (*o*-*C*H$_3$). FT-IR (neat): $\bar{\nu}$ = 3146(w), 3106(w), 3076(w), 2915(m), 1607(m), 1553(w), 1482(s), 1448(m), 1371(s), 1338(m), 1292(m), 1233(s), 1165(w) (C=Se), 1125(w), 1033(s), 925(w), 852(s), 754(s), 688(s), 595(s), 569(s) cm^{-1}.

Synthesis of 8

Complex **8** can be prepared as a by-product during the synthesis of **7** in method **2**. Yield: 30% based on [(IMes)CuCl]. Mp: 277–279 °C (decomposed). Elemental analysis calcd (%) for $C_{42}H_{48}ClCuN_4$ (707.85): C, 71.26; H, 6.83; N, 7.91; found: C, 71.30; H, 6.87; N, 7.94. ^{1}H NMR (400 MHz, $CDCl_3$): δ = 7.00 (s, 4H, Im*H*), 6.89 (s, 8H, C*H*$_{meta}$), 2.41 (s, 12H, C*H*$_{3para}$), 1.66 (s, 24H, C*H*$_{3ortho}$). ^{13}C NMR (100 MHz, $CDCl_3$): δ = 177.35 (*C*–Cu), 139.39, 134.53, 134.45, 129.16, 122.78 (Ar*C*), 21.18 (*p*-*C*H$_3$), 16.95 (o-*C*H$_3$). FT-IR (neat): $\bar{\nu}$ = 2912(m), 1604(m), 1542(w), 1483(s), 1400(m), 1266(s), 1230(s), 1163(m), 1069(m), 1036(m), 929(m), 857(s), 733(s), 641(m), 573(m) cm^{-1}.

Synthesis of 9

Method 1. Complex **9** can be prepared in the same manner as described for **1** using **IMes=Se** (0.100 g, 0.260 mmol) and $[Cu(CH_3CN)_4]PF_6$ (0.097 g, 0.260 mmol) in methanol (5 mL). Yield: 80% (based on $[Cu(CH_3CN)_4]PF_6$).

Method 2. IMes=Se (0.100 g, 0.260 mmol) was treated with [(IMes)CuCl] (0.208 g, 0.520 mmol) and an excess of KPF_6 (0.239 g, 1.300 mmol) in acetone under refluxing conditions overnight to yield the desired product **9**. Yield: 68% (based on [(IMes)CuCl]. Mp: 259 °C (decomposed). Elemental analysis calcd (%) for $C_{42}H_{48}CuF_6N_4PSe_2$ (975.28): C, 51.72; H, 4.96; N, 5.74; found: C, 51.73; H, 4.97; N, 5.80. ^{1}H NMR (400 MHz, $CDCl_3$): δ = 7.36 (s, 4H, Im*H*), 7.04 (s, 8H, C*H*$_{meta}$), 2.37 (s, 12H, C*H*$_{3para}$), 2.10 (s, 24H, C*H*$_{3ortho}$). ^{13}C NMR (100 MHz, $CDCl_3$): δ = 142.28 (*C*=Se), 140.96, 134.70, 132.53, 129.88, 124.58 (Ar*C*), 21.35 (*p*-*C*H$_3$), 18.47 (*o*-*C*H$_3$). ^{31}P NMR ($CDCl_3$, 161 MHz): −157.59 to −131.22 (sept, PF_6). ^{19}F NMR ($CDCl_3$, 376 MHz):

Open Access Article. Published on 18 September 2018. Downloaded on 11/8/2025 3:33:28 AM.
This article is licensed under a Creative Commons Attribution-NonCommercial 3.0 Unported Licence.

−74.72 to −72.83 (d, PF_6). FT-IR (neat): $\bar{\nu}$ = 1484(m), 1435(m), 1264(s), 1185(m) (C=Se), 1121(m), 834(s) (P–$F_{stretching}$), 731(s), 697(s), 549(s) cm^{-1}.

Synthesis of 10

Complex **10** can be prepared as a by-product during the synthesis of **9** and also **11** by method 2. Yield: 28% along with **9** and 25% along with **11** based on [(IMes)CuCl]. Mp: 238–240 °C (melting). Elemental analysis calcd (%) for $C_{42}H_{48}Cu_2F_6N_4P$ (817.36): C, 61.72; H, 5.92; N, 6.85; found: C, 61.73; H, 5.97; N, 6.84. ^{1}H NMR (400 MHz, $CDCl_3$): δ = 7.01 (s, 4H, Im*H*), 6.89 (s, 8H, CH_{meta}), 2.41 (s, 12H, CH_3para), 1.66 (s, 24H, CH_{3ortho}). ^{13}C NMR (100 MHz, $CDCl_3$): δ = 177.35 (*C*–Cu), 139.40, 134.52, 134.45, 129.16, 122.78 (Ar*C*), 21.18 (*p*-CH_3), 16.96 (*o*-CH_3). ^{31}P NMR ($CDCl_3$, 161 MHz): −157.59 to −131.21 (sept, *P*F_6). ^{19}F NMR ($CDCl_3$, 376 MHz): −74.73 to −72.84 (d, PF_6). FT-IR (neat): $\bar{\nu}$ = 2920(w), 1608(w), 1482(s), 1454(m), 1372(m), 1341(w), 1265(s), 1234(m), 1035(m), 840(s) (P–$F_{stretching}$), 734(s), 700(m), 557(s) cm^{-1}.

Synthesis of 11

Method 1. Complex **11** can be prepared in the same manner as described for **1** using **IPr=Se** (0.10 g, 0.213 mmol) and $[Cu(CH_3CN)_4]PF_6$ (0.040 g, 0.106 mmol) in methanol (5 mL). Yield: 78% (based on $[Cu(CH_3CN)_4]PF_6$).

Method 2. **IPr=Se** (0.100 g, 0.213 mmol) was treated with IMesCuCl (0.160 g, 0.426 mmol) and an excess of KPF_6 (0.19 g, 1.065 mmol) in acetone under refluxing conditions overnight to yield the desired product **11**. Yield: 70% based on [(IMes)CuCl]. Mp: 268–270 °C (decomposed). Elemental analysis calcd (%) for $C_{54}H_{72}CuF_6N_4PSe_2$ (1143.60): C, 56.71; H, 6.35; N, 4.90; found: C, 56.70; H, 6.37; N, 4.89. ^{1}H NMR (400 MHz, $CDCl_3$): δ = 7.43–7.39 (t, 2H, CH_{para}), 7.23–7.22 (d, 4H, CH_{meta}), 7.20 (s, 2H, Im*H*), 2.34–2.28 (sept, 4H, ^{i}PrC*H*), 1.20–1.19, 1.12–1.10 (d, 24H, CH_3). ^{13}C NMR (100 MHz, $CDCl_3$): δ = 155.76 (*C*=Se), 145.79 (Im*C*), 133.11, 131.11, 124.61, 123.37 (Ar*C*), 29.22 (^{i}Pr*C*H), 24.95, 23.44 (*C*H_3). ^{31}P NMR ($CDCl_3$, 161 MHz): −157.59 to −131.21 (sept, PF_6). ^{19}F NMR ($CDCl_3$, 376 MHz): −74.82 to −72.82 (d, PF_6). FT-IR (neat): $\bar{\nu}$ = 2962(m), 2867(m), 1558(w), 1463(s), 1420(m), 1345(s), 1265(m), 1212(w), 1181(m) (C–Se), 1120(w), 1060(m), 937(m), 839(s) (P–$F_{stretching}$), 803(w), 737(s), 555(s) cm^{-1}.

Synthesis of 12

CuI (0.50 g, 0.263 mmol) and excess of PPh_3 (1.38 g, 0.526 mmol) were mixed together in acetonitrile (20 mL) and allowed to stir at 85 °C overnight to yield a colourless clear solution, which upon cooling to room temperature gave, **12**. Yield: 82% (based on CuI). Mp: 221–223 °C (melting). Elemental analysis calcd (%) for $C_{72}H_{60}Cu_4I_4P_4$ (1810.94): C, 47.75; H, 3.34; found: C, 47.80; H, 3.37. ^{1}H NMR (400 MHz, $CDCl_3$): δ = 7.30–7.25 (m, 3H, Ar*H*), 7.17–7.13 (m, 2H, CH_{ortho}). ^{13}C NMR (100 MHz, $CDCl_3$): δ = 134.09, 133.94, 133.79, 133.58, 129.46, 128.47, 128.38 (Ar*C*). ^{31}P NMR ($CDCl_3$, 161 MHz): −4.96 (s, *P*Ph_3). FT-IR (neat): $\bar{\nu}$ = 1677(w), 1562(w), 1475(m), 1429(s), 1212(w), 1178(m), 1093(m), 1025(w), 995(w), 744(s), 691(s), 521(m) cm^{-1}.

Synthesis of 13

Method 1. Complex **12** (0.26 g, 0.143 mmol) and **Ebis** (0.10 g, 0.287 mmol) were mixed together and evacuated for 10 minutes under high *vacuo*. Subsequently, acetonitrile (5 mL) was added and stirred at 85 °C for 12 h to yield a clear colourless solution, which upon cooling to ambient temperature gave **13**. Yield: 75% (based on **12**).

Method 2. CuI (0.05 g, 0.299 mmol) and PPh_3 (0.15 g, 0.599 mmol) were mixed together in acetonitrile (5 mL) and allowed to stir at 85 °C for 3 h. To this clear solution, **Ebis** (0.10 g, 0.299 mmol) was added and was further stirred under reflux for 12 h to obtain a clear solution, which upon cooling to room temperature yielded **13**. Mp: 220–222 °C (decomposed). Elemental analysis calcd (%) for $C_{10}H_{14}Cu_2I_2N_4Se_2$ (729.06): C, 16.47; H, 1.94; N, 7.68; found: C, 16.43; H, 1.97; N, 7.64. ^{1}H NMR (400 MHz, $CDCl_3$): δ = 6.80–6.79 (d, 2H, Im*H*), 6.76 (d, 2H, Im*H*), 4.57 (s, 4H, CH_2–CH_2), 3.66 (s, 6H, CH_3). ^{13}C NMR (100 MHz, $CDCl_3$): δ = 155.73 (*C*=Se), 119.95, 119.75 (Im*C*), 47.22 (*C*H_2–*C*H_2), 37 091 (*C*H_3). FT-IR (neat): $\bar{\nu}$ = 2932(m), 1679(s), 1561(m), 1479(m), 1436(m), 1405(m), 1244(m), 1180(m) (C=Se), 1115(s), 1046(m), 924(w), 808(m), 751(w), 717(s), 690(s), 533(s) cm^{-1}.

Synthesis of 14

Method 1. Complex **14** was synthesized by the same method as described for **13** using **12** (0.22 g, 0.123 mmol) and **Ebpis** (0.10 g, 0.247 mmol). The successive addition of excess NH_4BF_4 (0.13 g, 1.235 mmol) to the reaction mixture produced a clear solution after 12 h. The reaction mixture was filtered and concentrated *in vacuo* to isolate **14**. Yield: 78% (based on **12**).

Method 2. CuI (0.05 g, 0.299 mmol) and PPh_3 (0.15 g, 0.599 mmol) were mixed together in acetonitrile (5 mL), and allowed to stir at 85 °C for 3 h. To the resulting clear solution, **Ebpis** (0.12 g, 0.299 mmol) and NH_4BF_4 (0.06 g, 0.599 mmol) were added then stirred under refluxing conditions for 12 h to obtain an orange precipitate. Upon cooling to room temperature **14** was obtained. Mp: 229–231 °C (decomposed). Elemental analysis calcd (%) for $C_{21}H_{33}B_1Cu_1F_4N_6Se_3$ (756.75): C, 33.33; H, 4.40; N, 11.11; found: C, 33.30; H, 4.37; N, 11.14. ^{1}H NMR (400 MHz, $CDCl_3$): δ = 6.79–6.76 (m, 4H, Im*H*), 5.26–5.07 (m, 2H, N–C*H*), 4.60 (s, 4H, CH_2–CH_2), 1.34–1.32 (d, 12H, CH_3). ^{13}C NMR (100 MHz, $CDCl_3$): δ = 154.13 (*C*=Se), 120.38, 114.77, 50.96, 46.71, 21.95 (*C*H_3). ^{11}B{^{1}H} NMR (128.4 MHz, $CDCl_3$): δ = −0.99. ^{19}F{^{1}H} NMR (376.4 MHz, $CDCl_3$): δ = −154.02. FT-IR (neat): $\bar{\nu}$ = 3170(w), 3141(w), 2977(w), 1567(m), 1453(m), 1418(s), 1325(s), 1218(m), 1175(m) (C=Se), 1135(m), 1036(s) (B–$F_{stretching}$), 741(s), 684(s), 640(m), 518(m) cm^{-1}.

General synthetic procedure for the [3+2] cycloaddition of azides and terminal alkynes

The azide (1.0 mmol), alkyne (1.2 mmol), catalyst (1 mol%) and water (1 mL) were loaded. The solution was stirred at room temperature for 1 h and the conversion was followed by TLC to ensure the completion of the reaction. After the complete conversion water (5 mL) was added, followed by the addition of ethyl acetate (5 mL). The reaction mixture was allowed to stir at

Open Access Article. Published on 18 September 2018. Downloaded on 11/8/2025 3:33:28 AM.
This article is licensed under a Creative Commons Attribution-NonCommercial 3.0 Unported Licence.

room temperature for a further 5–10 minutes, after which the ethyl acetate layer was collected and the volatiles were evaporated to obtain the solid. The acquired solid was further washed with *n*-hexane and dried under *vacuo* to yield the desired product. The isolated 1,2,3-triazole products were characterized by ^{1}H NMR and ^{13}C NMR spectroscopy to confirm the product purity.

General procedure for the synthesis of C–Si bonding

The catalyst (1 mol%) was placed in an oven-dried Schlenk flask that was evacuated for 5 minutes then refilled with an argon gas. CH_3CN (1 mL) was added to the flask under argon, followed by terminal alkyne (1.0 mmol), hydrosilane (1.2 mmol) and pyridine (0.2 mmol). The resulting mixture was allowed to stir at 100 °C for 12 h. After completion of the reaction, a saturated aqueous NH_4Cl solution (10 mL) was added to the mixture and the aqueous phase was extracted with ethylacetate (5 mL × 3). The combined organic layer was washed with brine (10 mL) and then dried over anhydrous sodium sulfate. Filtration and evaporation of the solvent followed by column chromatography on silica gel gave the corresponding product.

Results and discussion

The N-heterocyclic thione and selone ligands such as **IMes=S**, **IMes=Se**, **IPr=Se**, **Ebis** and **Ebpis** were synthesized in fairly good yields from their corresponding imidazolium salts using elemental chalcogen powders in the presence of potassium carbonate.[7k,l] These organochalcogen ligands were demonstrated as promising ligands for investigating the coordination abilities with copper metal. The copper(I) complexes isolated herein can be organized in three different categories such as neutral monomeric copper(I) complexes, cationic monomeric copper(I) complexes, neutral 2D copper(I) sheets and cationic 2D copper(I) sheets.

Neutral mononuclear copper(I) complexes **1–5** were synthesized by treating copper(I) halides with one equivalent of IMes=E in methanol (Scheme 1). The monomeric copper(I) complexes **1–5** were isolated in excellent yield. The crystalline solids **1–5** are only soluble in hot acetonitrile and in DMSO. The formation of these compounds was established by elemental analysis, FT-IR, multi nuclear NMR spectroscopy, UV-vis and single crystal X-ray diffraction techniques. In ^{1}H NMR, the aryl hydrogens were slightly downfield shifted upon complexation, while the imidazole hydrogens were largely downfield shifted due to hydrogen bonding interactions. The C=E signal in ^{13}C NMR was shifted up-field by 5–10 ppm due to the decrease in the π-acceptance nature of the carbene carbon upon complexation. The FT-IR spectra of molecules **1–5** show the existence of the C=E stretching frequency at 1163–1167 cm^{-1}, which is in agreement with the complex formation.

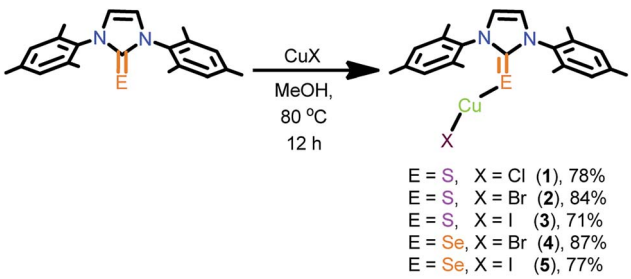

Scheme 1 Synthesis of **1–5**.

The solid state structures of **1–5** were unambiguously determined by single crystal X-ray diffraction (Fig. 1). Complexes **1–5** crystallized in the monoclinic space group, $P2_1/c$. The crystallographic data for **1–5** are listed in table S1 (see ESI-1, table S1†) and the important bond parameters are listed in the figure caption. The molecular structures of **1–5** are isostructural and are neutral monomeric copper(I) chalcogenone complexes with a copper : chalcogen ratio of 1 : 1. The copper(I) centre in **1–5** is two-coordinate with one imidazole thione/selone and one halogen atom. Interestingly, the molecular structures of **1–5** are comparable with NHC analogues of [(IMes)CuX].[12,13]

Upon coordination, the C=S bond lengths (1.699(3) Å for **1**, 1.699(3) Å for **2**, 1.699(8) Å for **3**) and C=Se bond lengths (1.855(5) Å for **4**, 1.842(9) Å for **5**) were marginally increased related to their corresponding ligands (**IMes=S** (1.675(18) Å) and **IMes=Se** (1.830(6) Å)).[5] The E–Cu–X bond angle in molecules **1–5** lies between 159.60(4)–165.94(6)°, suggesting the quasi-linear arrangement around the metal centre.

Molecules **1–5** have quite strong C–H···Cl hydrogen bonds, and also moderately strong C–H···S and C–H···Se hydrogen bonding interactions in their solid state structures as evidenced by single crystal X-ray diffraction analysis (see ESI-1, Fig. S16,† Chart 4). Surprisingly, the molecular packing of **1** is not

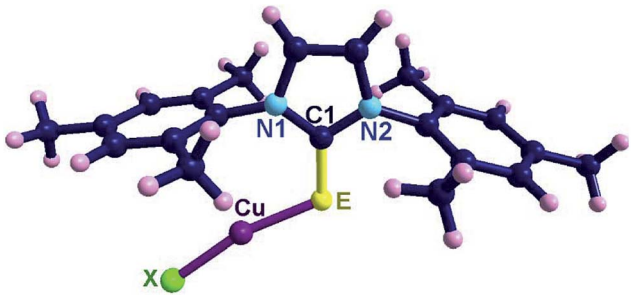

Fig. 1 Selected bond lengths (Å) and angles (°) for **1** (E = S, X = Cl): C(1)–S(1), 1.699(3), S(1)–Cu(1), 2.129(11), Cu(1)–Cl, 2.098(13), C(1)–S(1)–Cu(1), 109.13(11), N(1)–C(1)–N(2), 109.2(3), N(1)–C(1)–S(1), 129.6(3), N(2)–C(1)–S(1), 123.7(2), S(1)–Cu(1)–Cl, 165.94(6); for **2** (E = S, X = Br): C(1)–S(1), 1.699(3), S(1)–Cu(1), 2.135(9), Cu(1)–Br, 2.222(6), C(1)–S(1)–Cu(1), 108.61(10), N(1)–C(1)–N(2), 106.4(2), N(1)–C(1)–S(1), 129.6(2), N(2)–C(1)–S(1), 124.1(2), S(1)–Cu(1)–Br, 163.97(4); for **3** (E = S, X = I): C(1)–S(1), 1.699(8), S(1)–Cu(1), 2.142(3), Cu(1)–I, 2.385(16), C(1)–S(1)–Cu(1), 108.0(3), N(1)–C(1)–N(2), 105.4(7), N(1)–C(1)–S(1), 129.3(6), N(2)–C(1)–S(1), 125.3(6), S(1)–Cu(1)–I, 160.72(10); for **4** (E = Se, X = Br): C(1)–Se(1), 1.855(5), Se(1)–Cu(1), 2.241(11), Cu(1)–Br, 2.222(12), C(1)–Se(1)–Cu(1), 105.84(15), N(1)–C(1)–N(2), 106.6(5), N(1)–C(1)–Se(1), 129.3(4), N(2)–C(1)–Se(1), 124.1(4), Se(1)–Cu(1)–Br, 163.34(6); for **5** (E = Se, X = I): C(1)–Se(1), 1.842(4), Se(1)–Cu(1), 2.252(9), Cu(1)–I, 2.389(8), C(1)–Se(1)–Cu(1), 104.86(13), N(1)–C(1)–N(2), 105.9(4), N(1)–C(1)–Se(1), 129.5(3), N(2)–C(1)–Se(1), 124.6(3), Se(1)–Cu(1)–I, 159.60(4).

Open Access Article. Published on 18 September 2018. Downloaded on 11/8/2025 3:33:28 AM.
This article is licensed under a Creative Commons Attribution-NonCommercial 3.0 Unported Licence.

comparable with **2–5**. The hydrogen bonded polymeric chain through C(3)–H(3)···Cl (2.811(2) Å, 164.54(3)°) interactions are observed in **1**, and are marginally stronger than the C–H···Cl interactions reported for [(**IPr**=**S**)$BiCl_3$]·$CHCl_3$ (C(2)–H(2)···Cl(1); 2.871 Å, 145.32°).[7k] The solid state structure elucidated from the single crystal X-ray diffraction technique revealed the oppositely arranged molecular layers in molecule **1**, while all the other molecules (**2–5**) were arranged as AA′AA′AA′AA′AA′ (see ESI-1, Fig. S16 and S17†) in their solid states structures. In addition to this, an unusual C–H···S bonding was noticed in **2** (3.101(1) Å, 134.84(1)°) and **3** (3.044(3) Å, 136.51(7)°), while the very rare C–H···Se bonding was observed in **4** (3.158(1) Å, 132.74(3)°) and **5** (3.1241(1) Å, 132.134(3)°).[7k,14] The observed C–H···S interactions in **2** and **3** are quite weak compared to the interactions reported for [(**IPr**=**S**)$BiCl_3$]·$CHCl_3$ (H···S; 2.797 Å, 175.23°)[7k] and are stronger than the interactions reported for *N*,*N*′-dimethylthioformamide (H···S; 3.781(7) Å, 175.4(7)°).[15] Besides, the imidazole protons signal appeared to be shifted downfield (about 0.3 to 0.7 ppm) for molecules **1–5** due to the existence of hydrogen bonding (see ESI-1, S18†). Moreover, the C(1)–E(1)–Cu(1) bond angles are almost comparable. The existing E···H bond distances (3.044(3)–3.157(1) Å) and bond angles (132.13(3)–136.50(7)°) additionally support the moderately strong hydrogen bonding (Chart 4).[7k,16]

The cationic copper(I) complexes (**7–11**) were isolated in very good yields by treating **IMes**=**Se** (for **7** and **9**) and **IPr**=**Se** (for **11**) with [Cu(CH_3CN)$_4$]PF_6 in methanol (Scheme 2 and 3). Interestingly, these complexes can also be isolated in very good yield along with cationic NHC-copper(I) complexes **8** and **10** by the ligand transfer method from [(IMes)CuCl] (**6**).[17] The ligand exchange reaction signifies the better orbital overlap between the softer Lewis donor (NHC=Se) and the soft Cu(I) metal center.[18] Compounds **7**, **9** and **11** were crystallized at an ambient temperature. The compounds **8** and **10** were separated by handpicking them from the mixture and were purified by recrystallization from saturated dichloromethane solutions. The formation of **7**, **9** and **11** was established by elemental analysis, FT-IR, multinuclear NMR spectroscopy and single crystal X-ray diffraction techniques.

The PF_6 counter anion in molecules, **9** (834 cm^{-1}), **10** (840 cm^{-1}) and **11** (839 cm^{-1}) were confirmed by IR spectroscopy. The ^{31}P NMR displayed a septet for the presence of PF_6 (−131.21 to −157.59 ppm) ion and the ^{19}F NMR showed a doublet for the PF_6 (−72.82 to −74.82 ppm) ion. The C=Se was shifted upfield for **6** (178.98 ppm), for **7** (148.59 ppm), for **9** (142.28 ppm) and for **11** (154.21 ppm). Molecules **7** and **9** displayed (10–15 ppm) upfield shift after complexation, compared to their corresponding ligand (**IMes**=**Se**, 157.49 ppm); **11** showed an upfield shift around 8 ppm, compared to its ligand (**IPr**=**Se**, 162.14 ppm), suggesting the strong σ-donor nature of NHC=E over NHC.[7d,k,l]

The solid-state structures of **7**, **9** and **11** were confirmed by single crystal X-ray diffraction (Fig. 2). Complexes **7**, **9** and **11** crystallized in the monoclinic space group, $P2_1/n$ (for **7** and **9**), $C2/c$ (for **11**). The crystallographic data for **7**, **9** and **11** are given in Table S2 (see ESI†) and the important bond parameters are listed in the figure caption. The molecular structures of **7**, **9** and

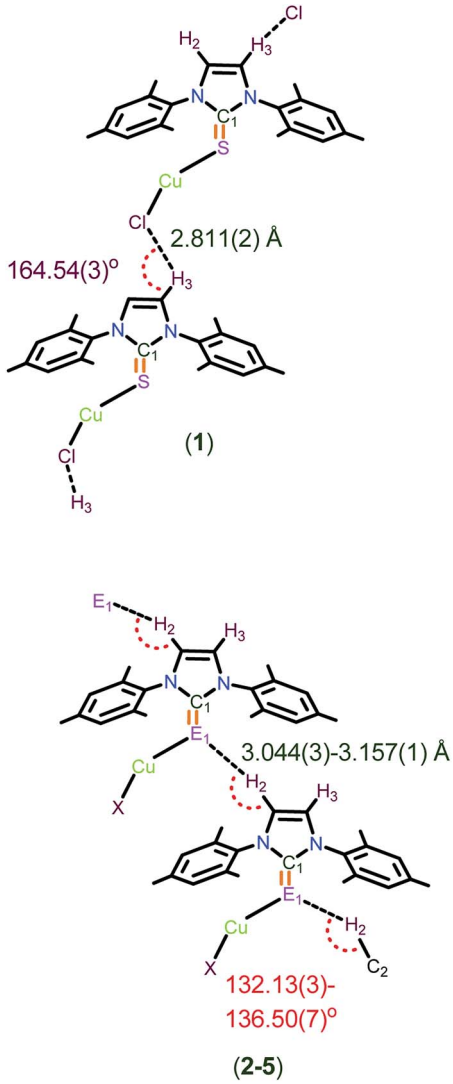

Chart 4 The representation of H(3)···Cl(1) bond distances in **1** and H(2)···E(1) bond distances and C(2)–H(2)–E(1) bond angles in molecules **2–5**.

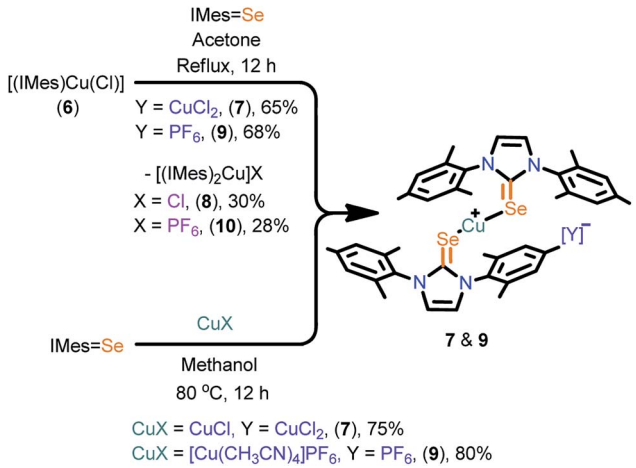

Scheme 2 Synthesis of **7** and **9**.

Open Access Article. Published on 18 September 2018. Downloaded on 11/8/2025 3:33:28 AM.
This article is licensed under a Creative Commons Attribution-NonCommercial 3.0 Unported Licence.

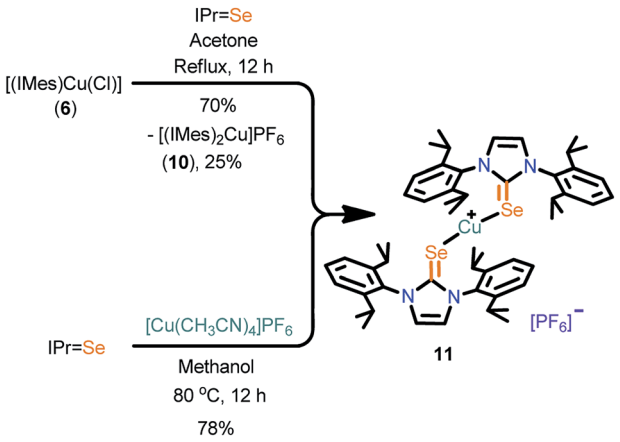

Scheme 3 Synthesis of **11**.

11 are cationic homoleptic mononuclear copper(I) selones. The copper(I) centre in **7**, **9** and **11** are two coordinate with two imidazoline-2-selones and its valence satisfied with one counter anion, particularly, $[CuCl_2]^-$ for **7**, $[PF_6]^-$ ion for **9** and **11**. The cationic salt **7** represent the first copper–NHC=E salt with loosely bound $[CuCl_2]^-$ salt.

The C=Se bond lengths in **7** (1.856(3) Å), **9** (1.853(3) Å) and **11** (1.849(3) Å) are considerably longer than in the corresponding ligands [**IMes=Se** (1.830(6) Å) and **IPr=Se** (1.822(4) Å)].[7d,k,l] The Se–Cu bond distances are similar and the Se–Cu–Se bond angles found in **7**, **9** and **11** are perfectly linear as reported by our group for linear copper(I) chalcogenones.[7d] Molecules **8** and **10** produced poor quality crystals but the bonding modes of NHC to the copper(I) metal centre were clearly established (see ESI†) by single crystal X-ray measurement.

Interestingly, the presence of the dichlorocuprate counter ion in **7** is responsible for the expected existence of the mononuclear complex as shown in Scheme 4. The NMR studies (^{1}H, ^{13}C, HMBC and HSQC) on molecule **7** and its spectral changes as compared with **1** suggest the existence of a mononuclear complex without any counter ion. To the best of our knowledge, this is one of the rare examples of metal–NHC=E that shows the dynamic equilibrium between homoleptic and heteroleptic species.

The 2D copper(I) layer **13** was isolated in good yield by treating $[(PPh_3)_3Cu_4I_4]$ with **Ebis**. **13** can also be isolated from the direct reaction between CuI, **PPh$_3$** and **Ebis** (Scheme 5). The two-dimensional ionic coordination polymer of **14** was isolated from the one-pot reaction between CuI, **PPh$_3$**, **Ebpis** and NH_4BF_4 or by treating **12** with **Ebpis** and NH_4BF_4 (Scheme 6). However, **12** was isolated in very good yield by treating CuI with an excess of **PPh$_3$** in acetonitrile.

These experiments signify the greater σ-donor strength of NHC=Se compared to PPh_3.[16] The formation of **13** and **14** was established by elemental analysis, FT-IR, multinuclear NMR spectroscopy and single crystal X-ray diffraction techniques. The FT-IR spectrum of **14** indicates the existence of the BF_4 counter ion (B–F$_{stretching}$, $\bar{\nu} = 1036\ cm^{-1}$), and was also approved by a signal at −0.99 ppm in ^{11}B NMR and a signal at −154.02 ppm in ^{19}F NMR. The carbene carbon signal in **13** (155.73 ppm) and **14** (154.13 ppm) was up-field shifted as expected after coordination to copper.[7d]

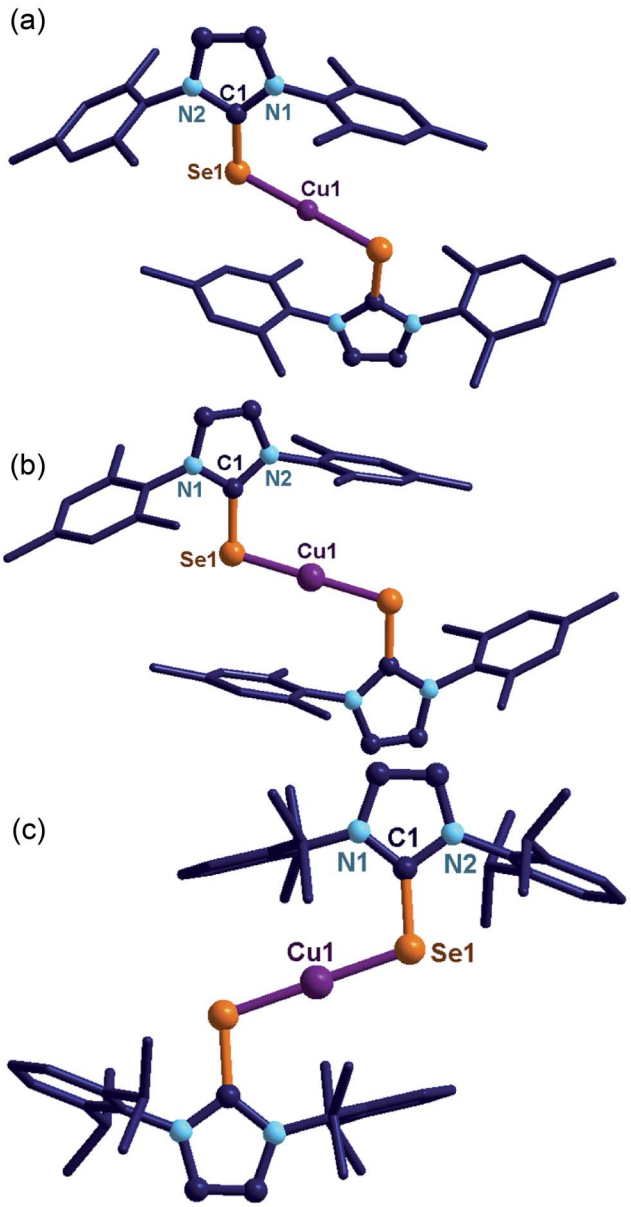

Fig. 2 (a) Molecular structure of **7**. Hydrogen atoms and dichlorocuprate counter ions have been omitted for clarity. Selected bond lengths (Å) and angles (°): C(1)–Se(1), 1.856(3), Se(1)–Cu(1), 2.253(3), Cu(2)–Cl(1), 2.090(2), C(1)–Se(1)–Cu(1), 105.24(9), N(1)–C(1)–N(2), 106.1(3), N(1)–C(1)–Se(1), 131.1(2), N(2)–C(1)–Se(1), 122.7(2), Se(1)–Cu(1)–Se(1′), 180.0. (b) The molecular structure of **9**. Hydrogen atoms and hexafluoro phosphate counter anions have been omitted for clarity. Selected bond lengths (Å) and angles (°): C(1)–Se(1), 1.853(3), Se(1)–Cu(1), 2.252(3), C(1)–Se(1)–Cu(1), 104.61(10), N(1)–C(1)–N(2), 106.0(3), N(1)–C(1)–Se(1), 123.0(2), N(2)–C(1)–Se(1), 130.9(2), Se(1)–Cu(1)–Se(2), 180.0. (c) The molecular structure of **11**. Hydrogen atoms and hexafluoro phosphate counter anions have been omitted for clarity. Selected bond lengths (Å) and angles (°): C(1)–Se(1), 1.849(3), Se(1)–Cu(1), 2.267(3), C(1)–Se(1)–Cu(1), 105.89(9), N(1)–C(1)–N(2), 105.7(2), N(1)–C(1)–Se(1), 122.7(2), N(2)–C(1)–Se(1), 131.6(2), Se(1)–Cu(1)–Se(2), 180.0.

Open Access Article. Published on 18 September 2018. Downloaded on 11/8/2025 3:33:28 AM.
This article is licensed under a Creative Commons Attribution-NonCommercial 3.0 Unported Licence.

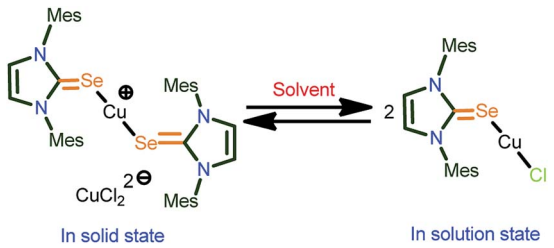

Scheme 4 Expected solution-state structure of **7** as suggested by NMR studies.

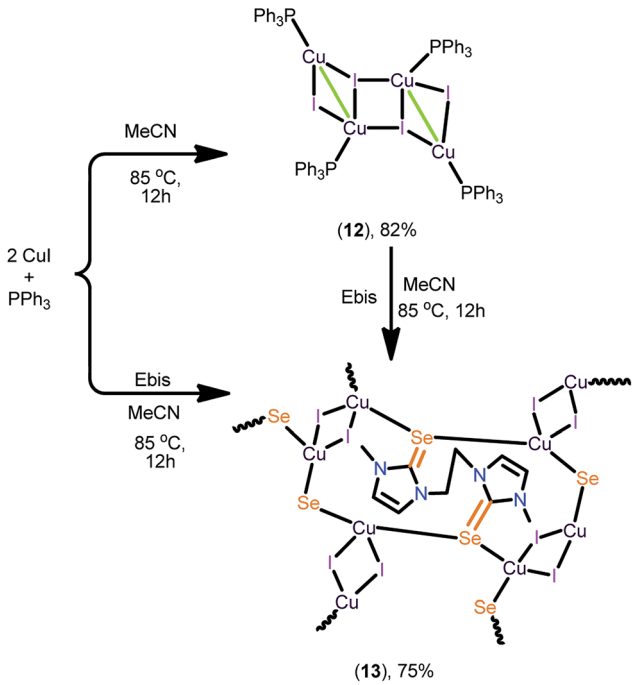

Scheme 5 Synthesis of **12** and **13**.

The solid-state structures of **12–14** were determined by the single crystal X-ray diffraction technique (Fig. 3 and 4). Molecule **12** crystallized in the monoclinic space group, $C2/c$, while **13** crystallized in the monoclinic space group, $P2_1/c$ and **14** crystallized in the tetragonal space group, $P4_12_12$. The crystallographic data for **12**, **13** and **14** are listed in Table S3 (see ESI†) and the important bond parameters are listed as figure captions.

The copper(I) centre in **12** shows two types of coordination environments, namely, tetra and penta with μ_2 and μ_3 bridging iodides. The coordination environment of the penta coordinated copper in **12** is fulfilled by three iodine atoms, one phosphine and one copper atom. The coordination environment of the tetra coordinated copper is fulfilled by two iodine atoms, one phosphorus and one copper atom. The μ_3 bridged iodine and copper distances are longer than the distance noted between the μ_2 bridged iodine with copper centres. The μ_3 bonded Cu–I distances (2.713(14) Å) are slightly longer than the μ_2 bonded Cu–I distances (2.645(14) Å). The Cu–P bond lengths

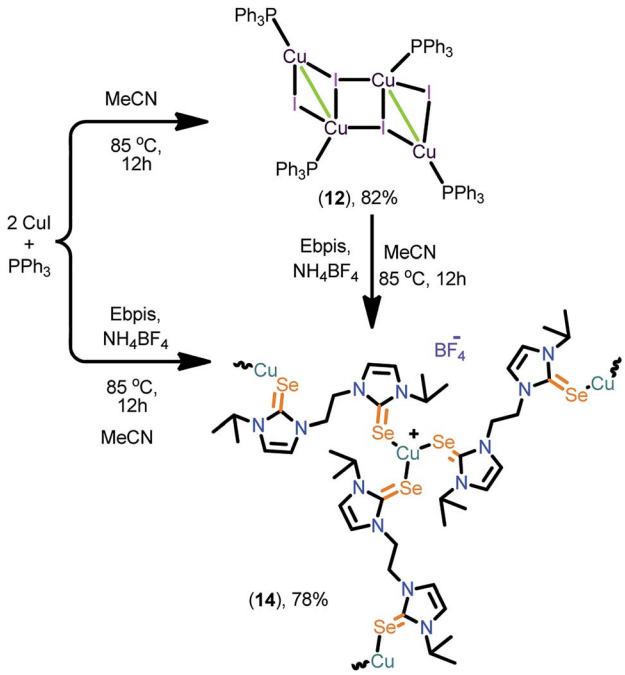

Scheme 6 Synthesis of **14**.

[Cu(1)–P(1), 2.248(2) Å, Cu(2)–P(2), 2.227(2) Å] are comparable. The Cu–Cu distance in molecule **12** is 2.843(19) Å, which is comparable with the sum of the van der Waals radii for copper (2.8 Å).[17]

Molecule **13** is a two-dimensional sheet consisting of a Cu_2I_2 core. Each Cu_2I_2 core is further connected by **Ebis** ligands to form an interesting 2D layer of **13** (see ESI-1, S47†). The copper(I) centre in **13** adopts a tetrahedral geometry (106.384(0)–

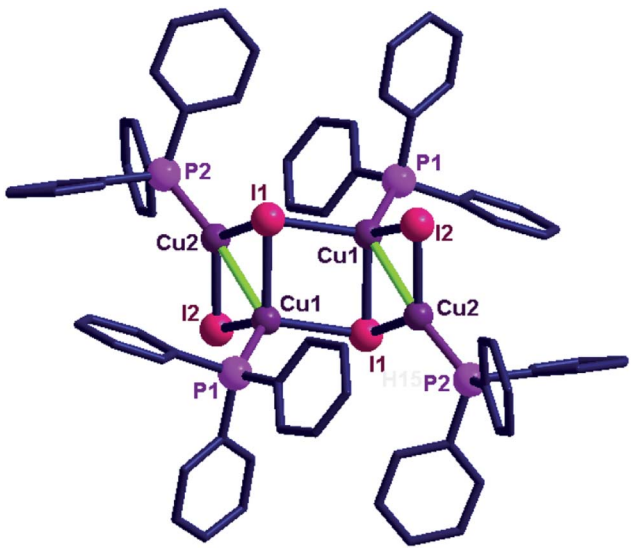

Fig. 3 Solid state structure of **12**. Selected bond lengths (Å) and angles (°): Cu(1)–P(1), 2.248(2), Cu(2)–P(2), 2.227(2), Cu(1)–Cu(2), 2.843(19), Cu(1)–I(1), 2.713(14), Cu(1)–I(2), 2.645(14), Cu(2′)–I(1), 2.590(14), Cu(2)–I(2), 2.533(14), Cu(1)–I(1)–Cu(2′), 105.86(4), Cu(1)–I(2)–Cu(2), 66.57(4), Cu(1′)–I(2)–Cu(2′), 64.72(2).

Open Access Article. Published on 18 September 2018. Downloaded on 11/8/2025 3:33:28 AM.
This article is licensed under a Creative Commons Attribution-NonCommercial 3.0 Unported Licence.

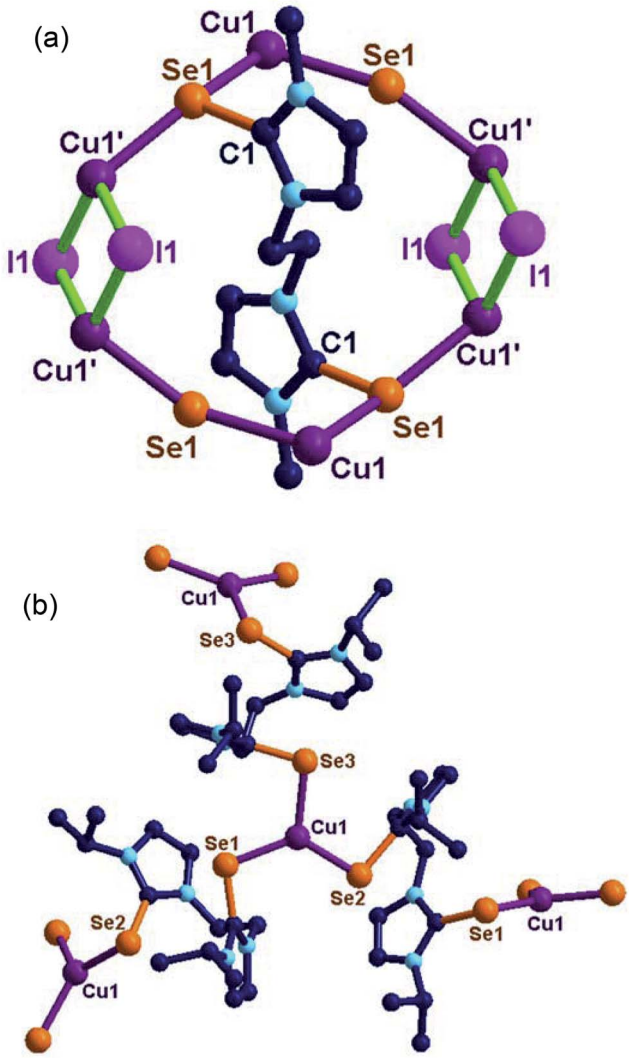

Fig. 4 (a) Solid-state structure of **13**. Selected bond lengths (Å) and angles (°): C(1)–Se(1), 1.867(7), Se(1)–Cu(1), 2.553(14), Cu(1)–I, 2.650(12), Cu(1′)–I, 2.660(13), C(1)–Se(1)–Cu(1), 95.3(2), C(1)–Se(1)–Cu(1′), 103.4(2), N(1)–C(1)–N(2), 106.8(6), N(1)–C(1)–Se(1), 127.3(5), N(2)–C(1)–Se(1), 125.9(5), Cu(1)–Se(1)–Cu(1′), 160.72(10). (b) Solid state structure of **14**. Selected bond lengths (Å) and angles (°): C(1)–Se(1), 1.859(5), Se(1)–Cu(1), 2.336(9), C(8)–Se(2), 1.874(5), Se(2)–Cu(1), 2.323(10), C(15)–Se(3), 1.842(10), Se(3)–Cu(1), 2.352(10), C(1)–Se(1)–Cu(1), 102.35(15), C(8)–Se(2)–Cu(1), 99.85(16), C(15)–Se(3)–Cu(1), 98.6(3), Se(1)–Cu(1)–Se(2), 126.86(4), Se(1)–Cu(1)–Se(3), 114.60(4), Se(2)–Cu(1)–Se(3), 118.49(4), N(1)–C(1)–N(2), 106.0(5), N(1)–C(1)–Se(1), 125.6(4), N(2)–C(1)–Se(1), 128.3(4), N(3)–C(8)–N(4), 106.0(5), N(3)–C(8)–Se(2), 127.1(4), N(4)–C(8)–Se(2), 126.9(4), N(5)–C(15)–N(6), 108.7(12), N(5)–C(15)–Se(3), 125.1(10), N(6)–C(15)–Se(3), 126.2(11).

113.20(1)°) with two selone units and with two iodides. The bridging Cu–I distance (2.650(12) Å to 2.660(13) Å) are in the expected range. The Se–Cu distance is (2.553(14) Å) considerably longer than that of **4**, **5**, **7**, **9**, **10** and **14**. This is rare structural evidence for the μ_2 bridging mode of bis-imidazolin-2-chalcogenone ligands.[6d,e,17b]

Molecule **14** exists as a two-dimensional sheet through tri-coordinated homoleptic copper selenide (114.60(4)° to 126.86(4)°). The geometry of the copper(I) centre in **14** can be described as trigonal planar. The coordination environment around copper(I) is satisfied by μ_3 bridging **Ebpis** ligands. The Se–Cu distances in **14** are slightly elongated (2.323(10)–2.336(9) Å) due to the formation of extended coordination (see ESI-1, S48†).

The solution-state UV-vis absorption spectra of **1–14** were measured in CH_3CN at 25 °C (Fig. 5(a)–(f)). As shown in Fig. 5, the solution-state UV-vis absorption spectra of **1–14** were measured in CH_3CN at 25 °C (Fig. 5(a)–(f)). The solid-state UV-visible spectra of **1–14** are broad compared to their solution-state UV-visible spectra, mainly due to the molecular association in the solid state. The selone derivatives (**4** and **5**) of **IMes=E** show a slight bathochromic shift compared to the thione derivatives (**1–3**). Besides, all the complexes had absorption at higher wavelengths than the corresponding ligands **IMes=S** (243, 273 nm), **IMes=Se** (246 and 290 nm).[7k] The solution-state spectra are almost identical except for **5**, which shows a slight red shift. Molecules **8** and **10** show slight red shifts for n–π* transitions, while in the solid-state π–π* and n–π* transitions are merged together to show a broad absorption range to support the molecular association. Upon coordination, **7**, **9** and **11** showed shifts by about 50 nm for n–π* transitions due to the influence of the selone moiety. The solid-state UV-visible spectra of complexes **12–14** display broad signals in the range of 200–400 nm, while the same appeared to be distinct signals for π–π*and n–π* transitions in the solution-state UV-visible

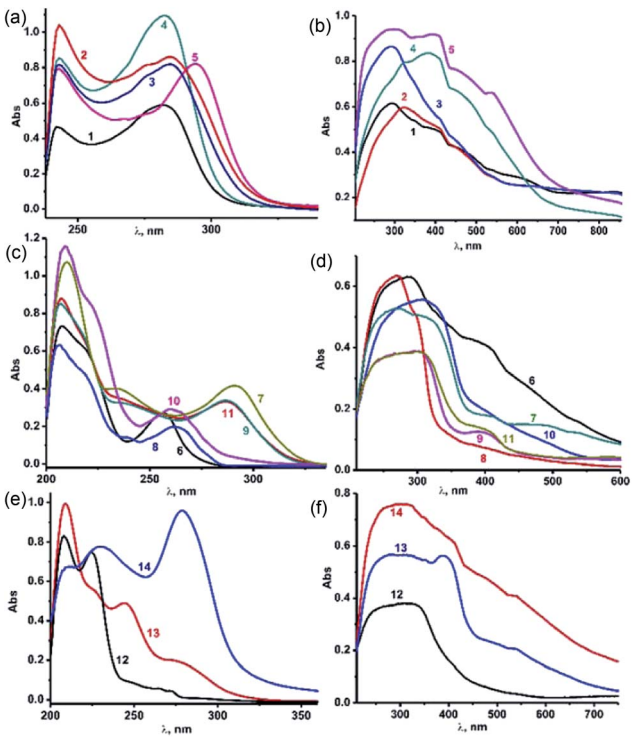

Fig. 5 (a) Solution UV-vis spectra of complexes **1–5** in acetonitrile at 298 K with 1.2 × 10^{-5} M solutions. (b) Solid-state UV-vis spectra of complexes **1–5** at 298 K. (c) Solution UV-vis spectra of complexes **6–11** in acetonitrile at 298 K with 1.2 × 10^{-5} M solutions. (d) Solid state UV-vis spectra of complexes **6–11** at 298 K. (e) Solution UV-vis spectra of complexes **12–14** in acetonitrile at 298 K with 1.2 × 10^{-5} M solutions. (f) Solid state UV-vis spectra of complexes **12–14** at 298 K.

Open Access Article. Published on 18 September 2018. Downloaded on 11/8/2025 3:33:28 AM.
This article is licensed under a Creative Commons Attribution-NonCommercial 3.0 Unported Licence.

study. The absorption bands at 274 nm (for **13**) and 278 nm (for **14**) can be assigned to ligand–metal charge transfer.

The applications of the newly isolated catalysts (**1–5**, **7**, **9** and **11–14**) were investigated for the click reaction of azides with terminal alkynes. The well-known catalysts, such as [(IMes)CuCl] (**6**) together with the homoleptic NHC derivatives such as $[(IMes)_2Cu][Cl]$ (**8**) and $[(IMes)_2Cu][PF_6]$ (**10**) were also tested for comparison.[18] Although various bis-NHC, abnormal-NHC and few chalcogenone based ligands were also employed in CuAAC reactions, a detailed study comparing the catalytic efficiency of the NHC=E supported copper(I) complexes with NHC or phosphine supported Cu(I) has not been conducted.[7,20,21] Therefore, we have demonstrated the click catalysis using the NHC=E supported copper(I) complexes and compared the catalytic efficiency with NHC and phosphine supported copper(I) complexes for the first time. To the best of our knowledge, the significance of ancillary ligands such as PPh_3, NHC, NHC=S and NHC=Se have never been compared in any catalysis.[7d,e,8,20]

The catalytic reactions were carried out under neat conditions at room temperature (Scheme 7) (Fig. 6). Notably, the catalysts **1–5**, **6**, **8** and **10** (Entries 1–5) gave very good conversion (70–92%) within 1 h;[19] the linear copper(I) chalcogenones (**7**, **9** and **11**) gave moderate yields (68–76%, Entries 7, 9 and 11).

The coordination polymers (**13** and **14**) (68–75%, Entries 13–14) were found to be as active as linear chalcogenones in this catalysis. The phosphine-based copper(I) iodide (**12**) was found to be the most efficient (95%, Entry 12) among all the catalysts isolated herein. Catalysts **3**, **6** and **12** were found to be the most efficient in this catalysis (90–95%, Entries 3, 6 and 12) among all the isolated catalysts **1–14** (Chart 5). The effect of the ligand for this transformation was investigated by carrying out the experiments with only copper(I) chloride (Entry 15) or copper(I) iodide (Entry 16) and a poor yield was obtained. The *in situ* generated catalysts gave considerable yields (52–58%, Entries 17 and 19). The IMes.HCl addition to CuCl also produced a decent yield (45%, Entry 18). Entries 15–19 show the significance of the presence of ligand for this reaction and indicate the prominence of a well-defined catalyst. The decrease in the quantity of catalyst **12** to 0.5 mol% led to the isolation of 90% yield but after 4 h (Entry 20). Thus, catalysts **3**, **6** and **12** seem to be the efficient catalysts.

In order to investigate the effect of solvent in this reaction, the better catalysts (**3**, **6** and **12**) were subjected to click catalysis in various polar solvents as described in Fig. 7. Virtually identical output was perceived for all three catalysts in different solvents, but water was found to be a better choice (Entry 1).

All three catalysts **3**, **6** and **12** were examined for the substrate scope in water (Scheme 8, Chart 6). Interestingly, the substantial discrepancies in reactivity were not observed. The catalysts **3**, **6** and **12** were remarkably efficient to produce 18 different heterocyclic compounds.

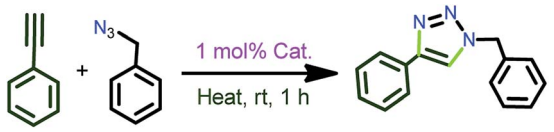

Scheme 7 [3+2] cycloaddition of benzylazide with phenyl acetylene.

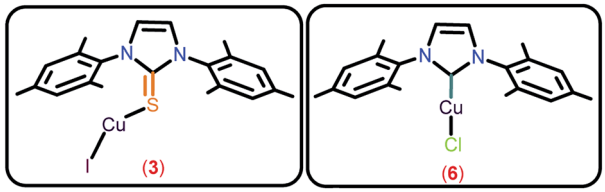

Chart 5 Catalysts used for the substrate scope in click catalysis.

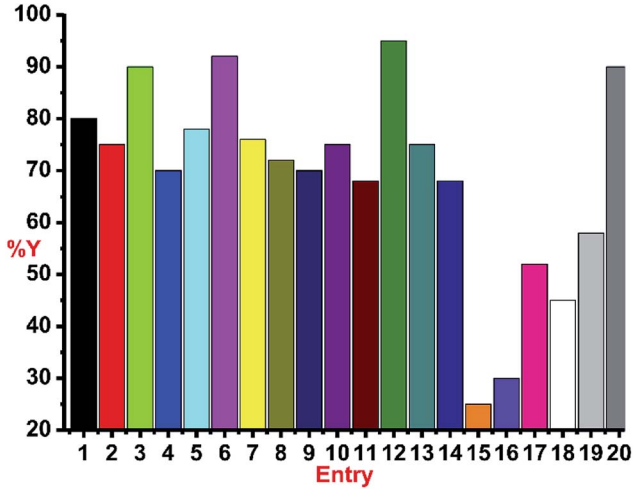

Fig. 6 The screening of catalysts **1–14** in click catalysis. Reaction conditions: phenyl acetylene (1.2 mmol), benzyl azide (1.0 mmol), catalyst (1 mol%) and neat conditions at RT. Entries: 15, CuCl only; 16, only CuI; 17, IMes=S and CuCl; 18, IMes.HCl and CuCl; 19, PPh_3 and CuI; 20, 0.5 mol% 12 for 4 h; %Y, %isolated yield by column chromatography.

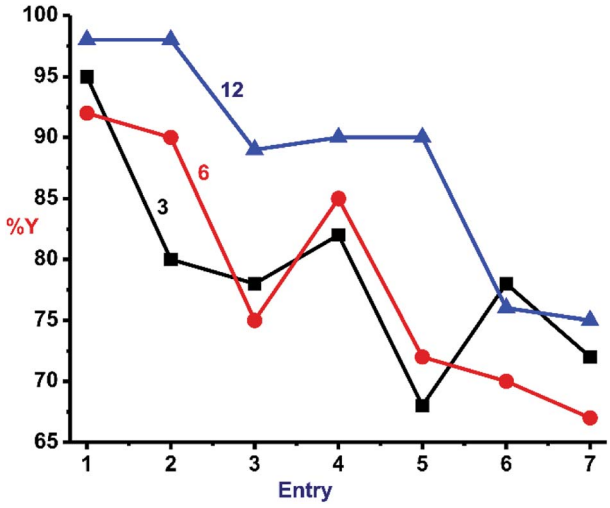

Fig. 7 Solvent screening in various solvents using catalysts **3** (black), **6** (red) and **12** (green); reaction conditions: phenylacetylene (1.2 mmol), benzylazide (1.0 mmol), catalyst (1 mol%) and solvent at RT. Entries: 1, in water; 2, in DMSO : water; 3, in THF : water; 4, in ^{t}BuOH : water; 5, in ^{t}BuOH; 6, in DMSO; and 7 in THF. % Y, % isolated yield by column chromatography.

Open Access Article. Published on 18 September 2018. Downloaded on 11/8/2025 3:33:28 AM.
This article is licensed under a Creative Commons Attribution-NonCommercial 3.0 Unported Licence.

Scheme 8 [3+2] cycloaddition of arylazides with terminal alkynes.

The plausible mechanistic pathway through which the thione/selone supported copper(I) complex proceeds, the click catalysis, has been displayed in chart 7[22]

The copper(I) catalyst is expected to form an intermediate **A** by coordinating with both terminal alkyne and azide (Chart 7).

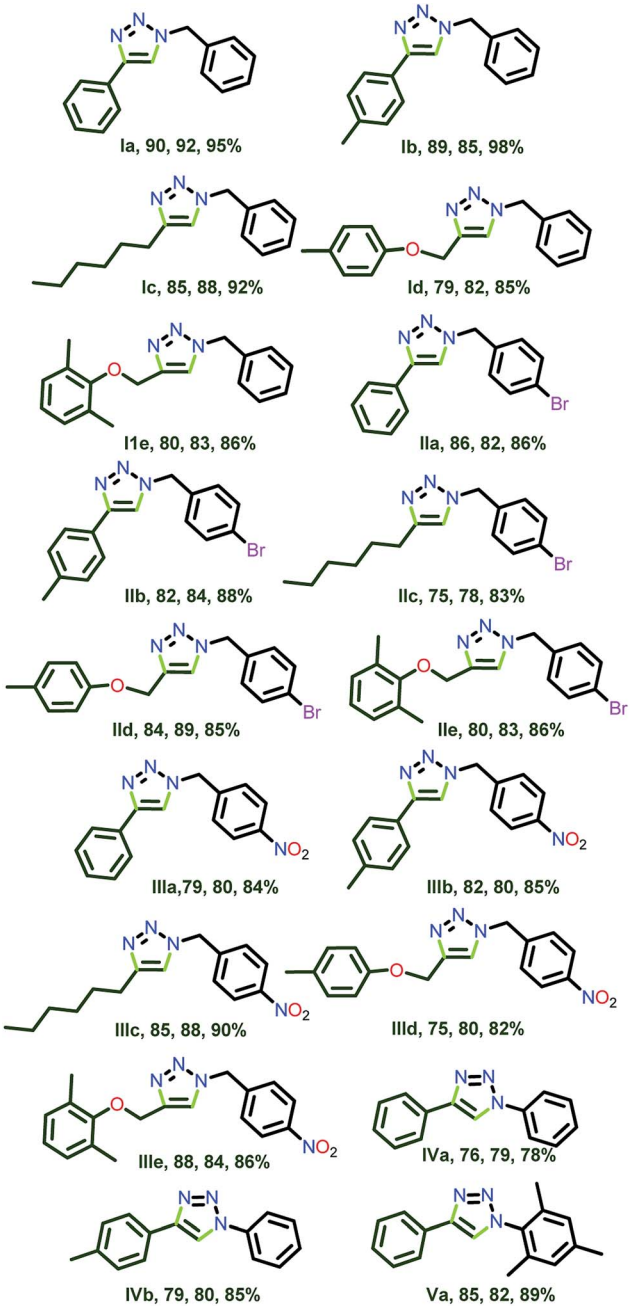

Chart 6 1,2,3-Triazoles isolated by click catalysis by **3**, **6** and **12** in water (see ESI-2, Table S2-1†).

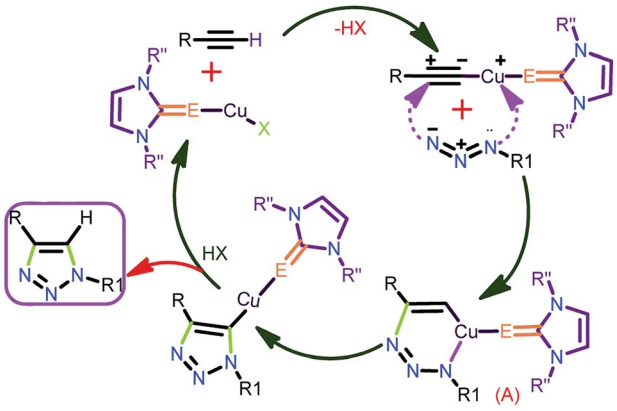

Chart 7 Plausible mechanisms for the Huisgen coupling reaction by catalyst **3**.[22]

Followed by the successive reproduction of catalyst to yield the desired 1,2,3-triazoles.

It is worth stating that the steric hindrance in molecules **7**–**11** and **13**–**14** has a major influence in constructing the intermediate **A**, which disfavours the product formation compared to catalysts **3** and **6**. The reasonably less steric hindrance exists at the metal centre in **3** due to the localization of the metal centre away from NHC *via* the thione, favouring the formation of the intermediate **A** in addition to the easy-leaving iodine attached to the metal (Chart 8). The greater efficiency of **12** was anticipated based on the presence of a greater number of electrophilic metal centers and also the more π-accepting (PPh_3) ligand, while **3** and **6** displayed relatively less activity because of the presence of the weakly π-accepting ligands attached to the metal.

Alkynylsilane derivatives are a noticeable class of structural motifs in organic synthesis as Si-masked synthetic intermediates, particularly for C–C and C–X (X = heteroatom) bond formation reactions.[23] The cross-dehydrogenative coupling of terminal alkynes and hydrosilanes has been studied with various metal salts such as H_2PtCl_6/I_2, CuCl/TMEDA (TMEDA = *N*,*N*,*N*′,*N*′-tetraethylenediamine), $LiAlH_4$, $Zn(SO_2CF_3)_2$/pyridine, MgO, and KNH_2/Al_2O_3.[24] However, the metal complexes-mediated cross-dehydrogenative coupling is limited, and the only example known so far is $M(\eta^2\text{-}Ph_2CNPh)(hmpa)_3$ (M = Yb or Ca, hmpa = hexamethylphosphoramide) (Chart 9).[25]

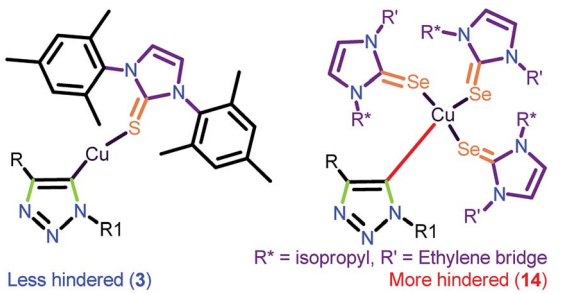

Chart 8 Expected steric hindrance at the metal centre in **3** and **14**.

Open Access Article. Published on 18 September 2018. Downloaded on 11/8/2025 3:33:28 AM.
This article is licensed under a Creative Commons Attribution-NonCommercial 3.0 Unported Licence.

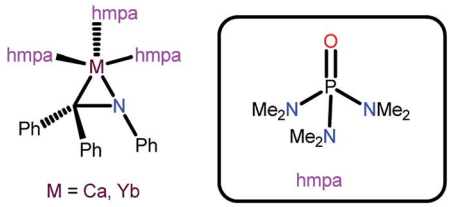

Chart 9 Catalysts used for the cross-dehydrogenative coupling of alkynes with hydrosilanes.

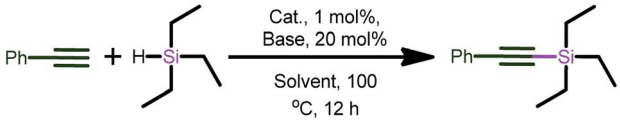

Scheme 9 Cross-dehydrogenative coupling of terminal alkynes with hydrosilanes.

Catalysts **1–14** were screened for the cross-dehydrogenative coupling of alkynes with hydrosilanes (Scheme 9 and Table 1). Initially, the dehydrogenative silylation was examined for suitable reaction conditions using phenylacetylene and triethylsilane (1 : 1.2 equivalents) in acetonitrile at 100 °C for 12 h without base (Entry 1) with 1 mol% catalyst **3** to produce 65% of the desired product. Interestingly, the addition of catalytic amounts (20 mol%) of organic base such as pyridine produced a quantitative yield (Entry 2). Nevertheless, catalysts **6** and **12** also gave the desired product in very good yield (Entries 13 and 14).

Catalyst **3** was utilized for this transformation to determine suitable conditions. The effect of base was investigated by employing the reaction with K_2CO_3 (Entry 4), KO^{t}Bu (Entry 5), NEt$_3$ (Entry 6) and KOH (Entry 7), but none of them produced quantitative yields (55–78% only). The effect of solvent on this reaction was studied by using CH_3OH (Entry 8), THF (entry 9), 1,4-dioxane (Entry 10) and toluene (Entry 11). The change in solvent did not favor the formation of the desired product. Subsequently, the influence of temperature on the reaction rate was investigated (Entry 12) by performing the reaction at room temperature. Even after extending the time for 24 h, the desired product formed was not satisfactory. Similarly, the significance of catalyst in this transformation was reviewed by performing this experiment without catalyst, and the yields were found to be inadequate (Entry 3). The plausible mechanism for the reaction is shown in Chart 10. The initial step may necessitate the nucleophilic attack to a copper center by alkyne to result transition state **A** followed by the nucleophilic attack to a silane to give the hypervalent silicon hydride via four membered transition-state **B** with a hydrogen bond, followed by the elimination of hydrogen to give the silane coupled product and regeneration of the catalyst.

Table 1 Catalyst **3**-mediated cross-dehydrogenative coupling reactions[a]

E	Solvent	Base	SMC[b]
1	CH_3CN	—	65%
2	CH_3CN	Pyridine	98%
3[c]	CH_3CN	Pyridine	10%
4	CH_3CN	K_2CO_3	57%
5	CH_3CN	KO^{t}Bu	78%
6	CH_3CN	NEt$_3$	55%
7	CH_3CN	KOH	68%
8	CH_3OH	Pyridine	12%
9	THF	Pyridine	19%
10	1,4-Dioxane	Pyridine	14%
11	Toluene	Pyridine	30%
12[d]	CH_3CN	Pyridine	62%
13[e]	CH_3CN	Pyridine	95%
14[f]	CH_3CN	Pyridine	92%

[a] Reaction conditions: phenylacetylene (0.40 mmol), triethylsilane (0.60 mmol), catalyst (1 mol%), base (20 mol%), solvent (1.0 mL); SMC: starting material conversion. [b] Percentage of conversion is based on GC (the given GC conversion values are the average of at least two independent measures). [c] Without catalyst. [d] Reaction at room temperature. [e] With catalyst **6**. [f] With catalyst **12**.

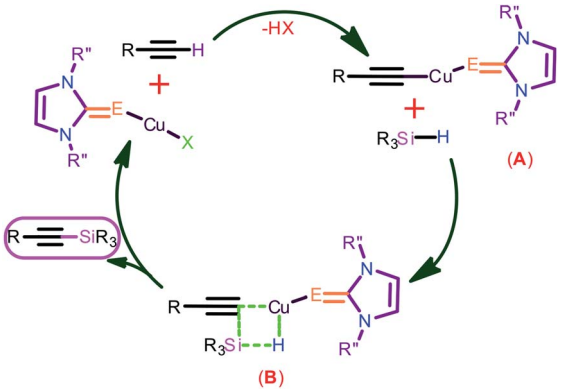

Chart 10 Possible mechanisms for the dehydrogenative coupling of silanes by catalyst **3**.

As presented in Chart 11 phenyl acetylene and 1-octyne were treated with triethylsilane, dimethylphenylsilane and over 90%

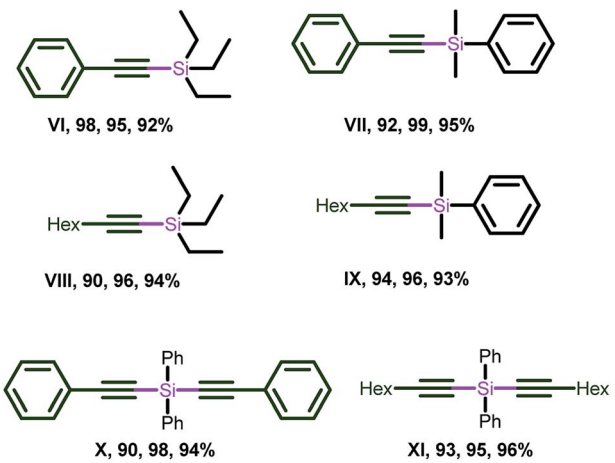

Chart 11 Alkynylsilanes isolated by **3**, **6** and **12**. Reaction conditions for **X** and **XI**: phenylacetylene (0.80 mmol), diphenylsilane (0.40 mmol), catalyst (1 mol%), base (20 mol%), solvent (1.0 mL). (See ESI-2, Table S2-2†).

Open Access Article. Published on 18 September 2018. Downloaded on 11/8/2025 3:33:28 AM.
This article is licensed under a Creative Commons Attribution-NonCommercial 3.0 Unported Licence.

yields were achieved (compounds **VI–IX**). Similarly, the double dehydrogenative coupling was carried out using diphenylsilane to afford the silicon-tethered diyene building blocks (**X–XI**) with very good yield. It is worth mentioning that the dehydrogenative coupling of alkynes with triphenyl silane led to the recovery of starting materials, which supports the unfavorable condition of the steric bulk of silane in this transformation.

Conclusions

Copper(I) complexes supported by NHC (for **6**, **8** and **10**), NHC=E (for **1–5**, **7**, **9**, **11**, **13** and **14**) and PPh_3 (for **12**) were synthesized and structurally characterized. The molecules **1–5** were isolated as rare mononuclear NHC=E supported neutral copper(I) chalcogenones. The molecules **7**, **9** and **11** were isolated by ligand exchange reaction between [(IMes)CuCl] and **6**, **8** and **10**. The synthetic methodology for **6**, **8** and **10** represents the first synthetic strategy to isolate copper chalcogenones from copper carbene derivatives. Complexes **7–11** display a perfectly linear geometry around the copper(I) center. Molecules **13** and **14** were isolated from the copper(I) phosphine iodide complex **12**. These newly isolated molecules **1–14** were used as catalysts for the [3+2] cycloaddition of azides with terminal alkynes. The catalysts **3**, **6** and **12** were relatively more active for cycloaddition reactions. The cationic **3**, **6** and **12** were found to be efficient in the C–Si bond formation reaction. (i) The ligand exchange experiment signifies the higher σ-donor abilities of NHC=E. (ii) The PPh_3 based catalyst (**12**) is effective in click catalysis over NHC=E and NHC based catalysts. (iii) Less steric hindrance and more Lewis acidic metal centres facilitate the reaction. (iv) The efficiencies derived in this work are **12**> **3**> **6**> **1**= **2**= **4**= **5**> **7**= **8**= **9**= **10**= **11**= **13**= **14**. (v) The softer Lewis donor (NHC=E) seems to have better orbital overlap with the soft Cu(I) metal center than NHC or PPh_3. Investigations are currently in progress in our laboratory comparing NHC and NHC–analogous metal complexes in terms of stability and reactivity in organic transformations in order to reduce the reaction times and produce quantitative yields.

Conflicts of interest

There are no conflicts to declare.

Acknowledgements

We gratefully acknowledge the DST-SERB (EMR/2017/001211) for financial support. KS thank UGC for the fellowship.

Notes and references

1 (*a*) S. V. C. Vummaleti, D. J. Nelson, A. Poater, A. G. –Suárez, D. B. Cordes, A. M. Z. Slawin, S. P. Nolan and L. Cavallo, *Chem. Sci.*, 2015, **6**, 1895–1904; (*b*) M. K. Barman, A. K. Sinha and S. Nembenna, *Green Chem.*, 2016, **18**, 2534–2541; (*c*) M. Melaimi, R. Jazzar, M. Soleilhavoup and G. Bertrand, *Angew. Chem., Int. Ed.*, 2017, **56**, 10046–10068; (*d*) D. J. Nelson, F. Nahra, S. R. Patrick, D. B. Cordes, A. M. Z. Slawin and S. P. Nolan, *Organometallics*, 2014, **33**, 3640–3645.

2 For the catalytic reactions studied with both NHC–metal and NHC=E–metal: (*a*) M. M. Kimani, C. A. Bayse, B. S. Stadelman and J. L. Brumaghim, *Inorg. Chem.*, 2013, **52**, 11685–11687; (*b*) E. E. Battin, M. T. Zimmerman, R. R. Ramoutar, C. E. Quarles and J. L. Brumaghim, *Metallomics*, 2011, **3**, 503–512.

3 J. Choi, N. Kang, H. Y. Yang, H. J. Kim and S. U. Son, *Chem. Mater.*, 2010, **22**, 3586–3588.

4 (*a*) D. J. D. Wilson, S. A. Couchman and J. L. Dutton, *Inorg. Chem.*, 2012, **51**, 7657–7668; (*b*) K. Verlinden, H. Buhl, W. Frank and C. Ganter, *Eur. J. Inorg. Chem.*, 2015, **14**, 2416–2425; (*c*) D. J. Nelson, A. Collado, S. Manzini, S. Meiries, A. M. Z. Slawin, D. B. Cordes and S. P. Nolan, *Organometallics*, 2014, **33**, 2048–2058; (*d*) A. Liske, K. Verlinden, H. Buhl, K. Schaper and C. Ganter, *Organometallics*, 2013, **32**, 5269–5272.

5 (*a*) Y. Rong, A. A. Harbi, B. Kriegel and G. Parkin, *Inorg. Chem.*, 2013, **52**, 7172–7182; (*b*) V. Rani, H. B. Singh and R. J. Butcher, *Eur. J. Inorg. Chem.*, 2017, **31**, 3720–3728.

6 (*a*) C. A. Bayse and J. L. Brumaghim, *Biochalcogen Chemistry: The Biological Chemistry of Sulphur, Selenium and Tellurium*, ACS Symposium series 1152, American Chemical Society, Washington, DC, 2013, pp. 57–64; (*b*) M. M. Kimani, J. L. Brumaghim and D. VanDerveer, *Inorg. Chem.*, 2010, **49**, 9200–9211; (*c*) M. M. Kimani, H. C. Wang and J. L. Brumaghim, *Dalton Trans.*, 2012, **41**, 5248–5259; (*d*) M. M. Kimani, C. A. Bayse and J. L. Brumaghim, *Dalton Trans.*, 2011, **40**, 3711–3723; (*e*) M. M. Kimani, D. Watts, L. A. Graham, D. Rabinovich, G. P. A. Yap and J. L. Brumaghim, *Dalton Trans.*, 2015, **44**, 16313–16324; (*f*) B. S. Stadelman, M. M. Kimani, C. A. Bayse, C. D. McMillen and J. L. Brumaghim, *Dalton Trans.*, 2016, **45**, 4697–4711.

7 (*a*) E. Alvarado, A. C. Badaj, T. G. Larocque and G. G. Lavoie, *Chem.–Eur. J.*, 2012, **18**, 12112–12121; (*b*) J. Jin, H. –W. Shin, J. H. Park, J. H. Park, E. Kim, T. K. Ahn, D. H. Ryu and S. U. Son, *Organometallics*, 2013, **32**, 3954–3959; (*c*) N. Ghavale, S. T. Manjare, H. B. Singh and R. J. Butcher, *Dalton Trans.*, 2015, **44**, 11893–11900; (*d*) K. Srinivas, C. N. Babu and G. Prabusankar, *Dalton Trans.*, 2015, **44**, 15636–15644; (*e*) H. R. Kim, G. Jung II, K. Yoo, K. Jang, E. S. Lee, J. Yun and S. U. Son, *Chem. Commun.*, 2010, **46**, 758–760; (*f*) C. N. Babu, K. Srinivas and G. Prabusankar, *Dalton Trans.*, 2016, **45**, 6456–6465; (*g*) W. G. Jia, Y. B. Huang, Y. J. Lin and G. X. Jin, *Dalton Trans.*, 2008, 5612–5620; (*h*) Y. B. Huang, W. G. Jia and G. X. Jin, *J. Organomet. Chem.*, 2009, **694**, 86–90; (*i*) A. K. Sharma, H. Joshi, R. Bhaskar and A. K. Singh, *Dalton Trans.*, 2017, **46**, 2228–2237; (*j*) O. Prakash, K. N. Sharma, H. Joshi, P. L. Gupta and A. K. Singh, *Organometallics*, 2014, **33**, 2535–2543; (*k*) K. Srinivas, P. Suresh, C. N. Babu, A. Sathyanarayana and G. Prabusankar, *RSC Adv.*, 2015, **5**, 15579–15590; (*l*) K. Srinivas, A. Sathyanarayana, C. N. Babu and G. Prabusankar, *Dalton Trans.*, 2016, **45**, 5196–5209; (*m*) L. M. Zhang, H. Y. Li, H. X. Li, D. J. Young, Y. Wang and J. P. Lang, *Inorg. Chem.*, 2017, **56**, 11230–11243.

Open Access Article. Published on 18 September 2018. Downloaded on 11/8/2025 3:33:28 AM.
This article is licensed under a Creative Commons Attribution-NonCommercial 3.0 Unported Licence.

8 K. Srinivas and G. Prabusankar, *Dalton Trans.*, 2017, **46**, 16615–16622.
9 D. D. Perrin and W. L. F. Armarego, *Purification of laboratory chemicals*, Pergamon Press, London, 3rd edn, 1988.
10 O. V. Dolomanov, L. J. Bourhis, R. J. Gildea, J. A. K. Howard and H. Puschmann, *J. Appl. Crystallogr.*, 2009, **42**, 339–341.
11 (*a*) G. M. Sheldrick, *Acta Crystallogr., Sect. A: Found. Crystallogr.*, 1990, **46**, 467–473; (*b*) G. M. Sheldrick, *SHELXL-97, Program for Crystal Structure Refinement*, Universität Göttingen, Göttingen, 1997.
12 N. Parvin, S. Pal, S. Khan, S. Das, S. K. Pati and H. W. Roesky, *Inorg. Chem.*, 2017, **56**, 1706–1712.
13 W. Xie, J. H. Yoon and S. Chang, *J. Am. Chem. Soc.*, 2016, **138**, 12605–12614.
14 T. Steiner, *Angew. Chem., Int. Ed.*, 2002, **41**, 48–76.
15 H. Borrmann, I. Persson, M. Sandström and C. M. V. Stålhandske, *J. Chem. Soc., Perkin Trans. 1*, 2000, **1**, 393–402.
16 (*a*) M. R. L. Furst and C. S. J. Cazin, *Chem. Commun.*, 2010, **46**, 6924–6925; (*b*) N. M. Scott and S. P. Nolan, *Eur. J. Inorg. Chem.*, 2005, 1815–1828; (*c*) G. A. Blake, J. P. Moerdyk and C. W. Bielawski, *Organometallics*, 2012, **31**, 3373–3378.
17 (*a*) V. Charra, P. d. Frémont and P. Braunstein, *Coord. Chem. Rev.*, 2017, **293**, 48–79; (*b*) M. Slivarichova, R. C. d. Costa, J. Nunn, R. Ahmad, M. F. Haddow, H. A. Sparkes, T. Gray and G. R. Owen, *J. Organomet. Chem.*, 2017, **847**, 224–233.
18 (*a*) T. Nakamura, T. Terashima, K. Ogata and S. i. Fukuzawa, *Org. Lett.*, 2011, **13**, 620–623; (*b*) S. D. González, A. Correa, L. Cavallo and S. P. Nolan, *Chem.–Eur. J.*, 2006, **12**, 7558–7564.
19 S. D. González, E. C. E. Adán, J. B. Buchholz, E. D. Stevens, A. M. Z. Slawin and S. P. Nolan, *Dalton Trans.*, 2010, **39**, 7595–7606.
20 (*a*) R. Berg, J. Straub, E. Schreiner, S. Mader, F. Rominger and B. F. Straub, *Adv. Synth. Catal.*, 2012, **354**, 3445–3450; (*b*) S. C. Sau, S. R. Roy, T. K. Sen, D. Mullangi and S. K. Mandal, *Adv. Synth. Catal.*, 2013, **355**, 2982–2991; (*c*) S. Hohloch, C. Y. Su and B. Sarkar, *Eur. J. Inorg. Chem.*, 2011, 3067–3075; (*d*) F. Wang, H. Fu, Y. Jiang and Y. Zhao, *Green Chem.*, 2008, **10**, 452–456; (*e*) V. O. Rodionov, V. V. Fokin and M. G. Finn, *Angew. Chem., Int. Ed.*, 2005, **44**, 2210–2215; (*f*) S. I. Presolski, V. Hong, S.-H. Cho and M. G. Finn, *J. Am. Chem. Soc.*, 2010, **132**, 14570–14576; (*g*) S. Q. Bai, L. L. Koh and T. S. A. Hor, *Inorg. Chem.*, 2009, **48**, 1207–1213.
21 (*a*) F. Lazreg and C. S. J. Cazin, *Organometallics*, 2018, **37**, 679–683; (*b*) F. Lazreg, A. M. Z. Slawin and C. S. J. Cazin, *Organometallics*, 2012, **31**, 7969–7975.
22 (*a*) C. W. Tornøe, C. Christensen and M. Meldal, *J. Org. Chem.*, 2002, **67**, 3057–3064; (*b*) F. Himo, T. Lovell, R. Hilgraf, V. V. Rostovtsev, L. Noodleman, K. B. Sharpless and V. V. Fokin, *J. Am. Chem. Soc.*, 2005, **127**, 210–216.
23 (*a*) Y. R. Leroux, H. Fei, J.-M. Noël, C. Roux and P. Hapiot, *J. Am. Chem. Soc.*, 2010, **132**, 14039–14041; (*b*) R. Gleiter and D. B. Werz, *Chem. Rev.*, 2010, **110**, 4447–4488; (*c*) J. P. Brand, D. F. Gonzàlez, S. Nicolai and J. Waser, *Chem. Commun.*, 2011, **47**, 102–115; (*d*) B. M. Trost, M. T. Rudd, M. G. Costa, P. I. Lee and A. E. Pomerantz, *Org. Lett.*, 2004, **6**, 4235–4238.
24 (*a*) M. G. Voronkov, N. I. Ushakova, I. I. Tsykhanskaya and V. B. Pukhnarevich, *J. Organomet. Chem.*, 1984, **264**, 39; (*b*) H. Q. Liu and J. F. Harrod, *Can. J. Chem.*, 1990, **68**, 1100; (*c*) M. Itoh, M. Kobayashi and J. Ishikawa, *Organometallics*, 1997, **16**, 3068; (*d*) T. Tsuchimoto, M. Fujii, Y. Iketani and M. Sekine, *Adv. Synth. Catal.*, 2012, **354**, 2959; (*e*) M. Itoh, M. Mitsuzuka, T. Utsumi, K. Iwata and K. Inoue, *J. Organomet. Chem.*, 1994, **476**, c30; (*f*) T. Baba, A. Kato, H. Yuasa, F. Toriyama, H. Handa and Y. Ono, *Catal. Today*, 1998, **44**, 271.
25 (*a*) K. Takaki, M. Kurioka, T. Kamata, K. Takehira, Y. Makioka and Y. Fujiwara, *J. Org. Chem.*, 1998, **63**, 9265; (*b*) F. Buch and S. Harder, *Organometallics*, 2007, **26**, 5132.

 This journal is © The Royal Society of Chemistry 2018